A novel photo-labile caged peptide for the repairment of spinal cord injuries

Chunyu Lu

A thesis submitted to the
Faculty of Graduate and Postdoctoral Studies
In partial fulfillment of the requirements
For the MASc degree in Chemical Engineering

Department of Chemical and Biological Engineering
Faculty of Engineering

University of Ottawa

Abstract

Spinal cord injuries (SCI) are characterized by the inability of mature neurons to regenerate or repair by themselves. In an attempt to overcome the SCI, a novel photo-sensitive cyclic Arg-Gly-Asp-Ser (RGDS) peptide was synthesized using solid phase peptide synthesis (SPSS) to control 3T3 fibroblast cell attachment on hyaluronic acid (HA) hydrogel. The circular RGDS peptide was designed using RGDS sequence labeled with Anp group (3-Na-fmoc-amino-3-(2-nitrophenyl) propionic acid) at the N terminus. The peptide was photo-labile cyclic caged to shelter its bioactivity and UV light was used to make the peptide uncaged. Accuracy of the cyclic caged RGDS peptide was confirmed by high-performance liquid chromatography (HPLC) and mass spectrum (MS). The molecular weight of cyclic caged RGDS peptide was confirmed as 881 by matrix-assisted laser desorption/ionization (MALDI) and electrospray ionization (ESI) mass spectrum. Stability of the cyclic caged RGDS peptide under various pH conditions was verified by circular dichroism spectroscopy. The bioactivity of cyclic caged and uncaged RGDS peptide was tested by photo-controllable directing cell growth based on cell attachment study, cell counting study, and cell morphology study. Three dimensional model structures of cyclic caged and uncaged RGDS peptides were computed by Hyperchem program. The first order reaction theory of Anp uncaging reaction was confirmed by kinetic study. Bioactivity caging and uncaging property of the peptide was also fully confirmed by cell attachment study. This cyclic caged RGDS peptide would be a promising tool in cell patterning for repairing of SCI.

Résumé

Des blessures à la colonne vertébrale (BCV) sont caractérisées par l'incapacité des neurones matures de se régénérer ou de se réparer par eux-mêmes. Dans le but de remédier ce problème, un nouveau peptide photosensible Arg-Gly-Asp-Ser (RGDS) a été synthétisé en employant la technique de synthèse peptidique en phase solide (SPPS) pour contrôler l'attachement de fibroblaste 3T3 sur un gel d'acide hyaluronique. Le peptide RGDS circulaire a été conçu en utilisant une séquence de RGDS marquée avec un groupe Anp (3-Na-fmoc-amino-3-(2-nitrophenyl) acide propionique) au terminus - N. La bioactivité du peptide était protégée grâce à une enveloppe formée d'un groupe cyclique photosensible et l'exposition aux rayons UV permettait ensuite de libérer le peptide de cette enveloppe. La caractérisation du RGDS enveloppé s'est faite grâce à l'utilisation de chromatographie en phase liquide à haute performance (CLHP) et la spectroscopie de masse. Le poids moléculaire du peptide RGDS cyclique enveloppé a été déterminé comme étant 881 Da, et ce, par utilisation de désorption-ionisation laser assisté par matrice (MALDI) et l'ionisation par électronébuliseur (ESI). La stabilité du peptide RGDS cyclique enveloppé a été évaluée à différents pH par spectroscopie dichroïsme circulaire. La bioactivité du peptide RGDS cyclique enveloppée et non enveloppée a été mesurée par moyen de test d'attachement cellulaire guidé par rayon lumineux, par test de recensement cellulaire et par test de morphologie cellulaire. Des modèles trois dimensionnels du RGDS cyclique enveloppé et non enveloppé ont été conçus en utilisant le programme Hyperchem. La théorie de réaction de premier ordre pour la réaction de désenveloppage Anp a été confirmée par étude cinétique. La bioactivité des propriétés d'enveloppage et de désenveloppage du peptide a

également été confirmé par étude de fixation des cellules. Bref, ce peptide RGDS cyclique enveloppé pourrait bien être un outil innovateur pour la structuration cellulaire et, ainsi, la guérison des BCV.

Acknowledgements

I would like to express my sincere thanks and gratitude to my supervisor Dr. X. Cao and co-supervisor Dr. A. Basak for their constant supervision, professional guidance and altruistic help throughout the research work.

I also like to thank Uptal De for the help he rendered during the planning of the project, to Cathy Goubko for the help in experiment protocols, to Sharon Curtis for mass spectrum, to Yan Du for the help in cell culture, and to Mukunda Goswami for his help and suggestions.

I am extremely grateful to my parents, for their constant love, motivation, and encouragement.

Chunyu Lu

Table of Contents

List of Figures

Abbreviations

Abbreviation	Name
ADH	adipic acid dihydrazide
Adoa	8-amino-3,6-dioxaoctanoic acid
Anp	3-amino-3-(2-nitrophenyl) propionyl
ATP	adenosine 5´-triphosphate
BDNF	brain-derived neurotrophic factor
Boc	t-butyloxycarbonyl group
CD	circular dichroism
CNS	central nervous system
CNTF	ciliary neurotrophic factor
DCM	dichloromethane
DMEM	Dulbecco's modified eagle medium
DMF	dimethylformamide
DNA	deoxyribonucleic acid
ECM	extracellular matrix
EDC	1-Ethyl-3-(3-dimethylaminopropyl) carbodiimide
ESI-MS	electrospray ionization-mass spectrum
FBS	fetal bovine serum
FDA	food and drug administration

GP	glycerophosphate
HA	hyaluronic acid
HBTU	2-(1H-benzotriazole-1-yl)-1,1,3,3-tetramethyluronium hexafluorophosphate
IGF-I	insulin-like growth factor I
MALDI-MS	matrix-assisted laser desorption/ionization mass spectrum
PS	polystyrene
3D	3-dimensional

Chapter 1 Introduction

The spinal cord is a major bundle of nerves that extends from brain to the space between the first and second lumbar vertebrae. A spinal cord injury (SCI) is an injury to the spinal cord, which is caused by either trauma or compression. Some specific functions of the body are at risk of lost, such as sensory input and movement of certain parts of the body when damage occurs to spinal cord [1].

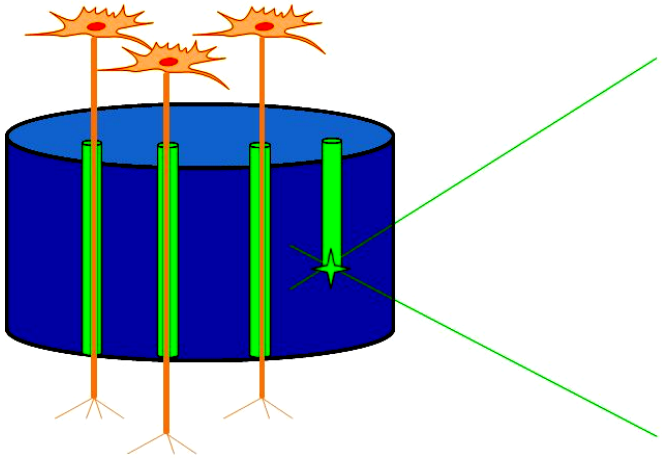

Figure 1. 3D micro-channel model showing to facilitate the axons growth guidance in damaged spinal cord by photo-labile caged cell-adhesion peptide

A 3-dimentional (3D) model as shown in Figure 1 would possibly be designed and realized to make the broken spinal cord connected to fix SCI. Caged peptide modified biomaterial would be mechanically made to a specific shape that could fit into the spinal column and connects the injured part of spinal cord. Various micro-channels could be built by using special irradiation such as two-photon laser, to activate the caged peptide [2]. Then the biomaterial, in these micro-channels, would be modified by active Arg-Gly-Asp-Ser (RGDS) peptide while the rest part of whole biomaterial would be modified by none-active RGDS. Active RGDS modified biomaterial would

provide ‘adhesive channels’ for axons to grow through to achieve directed growth. With the assistance of other necessary factors such as neurotrophic factors, the axons would hopefully be extended into the micro-channels from injured neurons on top of the material.

Chapter 2 Literature Review

2.1 Spinal Cord Injury and Repairing Methods

2.1.1 Over-view of SCI

The spinal cord is a major bundle of nerves that extends from brain to the space between the first and second lumbar vertebrae. A SCI occurs when there is damage to the spinal cord either from trauma, loss of normal blood supply, or compression from tumor or infection. As a result, specific functions are lost, such as sensory input and movement of certain parts of the body, when damage occurs to spinal cord [3]. SCI is classified into traumatic SCI and non-traumatic SCI. Traumatic SCI is caused by external physical impact, such as vehicle accidents, falls, or from violence that damages the spinal cord, while non-traumatic SCI is caused by a health condition, such as disease, infection, or a tumour [4].

A survey published by 'SCI Canada' (2013) indicated that there were over 86,000 people living with SCI and over 4,300 new SCI cases were reported each year in Canada [5]. Among these, approximately 51% were traumatic injuries and 49% were non-traumatic injuries. The estimated annual cost of traumatic injuries alone in Canada was approximately $3.6 billion dollars (CAD) and half of that was direct health care cost. To date, while extensive studies are being done to overcome the SCI, there is no widely accepted therapeutic modality bearing positive neurological outcome [6].

2.1.2 Promising Treatment Methods

2.1.2.1 Cellular Replacement

Cellular replacement therapy involves the transfer of stem/progenitor cells into the tissue of a target organ[7]. Usually, during traumatic SCI, both neurons and glia (cells providing support and

protection to for neurons) are lost. When cellular replacement treatment was applied to the injured spinal nerves, the substitutional nerve system could not realize the functions of lost cells. For example, motor neurons could be lost during the injury of the cervical spine. However, no matter how well these lesions were bridged, the lost neurons could not be regained [8].

A possible cellular replacement treatment was application of stem cells. Stem cells are superior for potential treatments for their self-renewal and differentiation characteristics. Stem cells present in the spinal column and their capability to regulate their population and functions made them an attractive choice for cellular replacement. It was recently shown that neural stem cells existed in non-human primates and humans [8]. In addition, it has also been reported that stem cells could continually divide in the adult brain and spinal cord throughout adult life [8]. Currently, several promising studies reported that mouse embryonic stem cells were used to repair SCI in mouse model. Oligodendrocytes derived from retinoic acid-induced embryonic stem cells were found to demonstrate myelinated axons *in vitro* which suggested that embryonic stem cell-derived oligodendrocytes had potential to replace myelin following SCI [9]. Billon *et. al.* reported a similar approach to efficiently produce neural precursor cells and oligodendrocytes from genetically modified embryonic stem cells [10]. Another stem cell transplantation study carried out *in vivo* demonstrated that embryonic stem cell-derived motor neuron effectively increased the chance of transplanted axons extending out of the spinal cord into ventral roots. In addition, these transplant-derived axons were physiologically active, successfully reached muscle, formed neuromuscular junctions, and mediated partial recovery from paralysis [11]. Significantly, the embryonic stem cells were also found to be able to survive for more than 50 days *in vivo* within injured spinal cord, which suggested the achievability of long term treatment of SCI [12].

Previous studies also demonstrated that human embryonic stem cells were directed toward

multipotent neural precursors, motor neurons, and oligodendrocytes progenitor cells [12]. In addition, Gabriel reported that oligodendrocytes progenitor cells were also differentiated into mature oligodendrocytes *in vitro* as well as *in vivo* [13]. These differentiated cells were demonstrated to be capable of myelinating axons and improving the recovery of forelimb function following transplantation to the spinal cord of myelin-deficient mice and adult rats *in vivo* [14].

Stem cell therapy showed great promises for SCI repairs, but their true potential has not been clearly explored and the potential risks (stem cell failure, organ injury, and infection) are still unclear[15]. In addition, there are also many unpredictable barriers such as ethical issues which must be addressed before this approach can be fully tested in clinical applications.

2.1.2.2 Neurotrophic Factor Delivery

Recent experimental advances suggested that following traumatic SCI, some morphological and functional recovery were achieved when appropriate treatments, such as certain neurotrophic factors were provided [16]. Neurotrophic factors attracted considerable attention because they were known to possess the capability of facilitating nervous system development, axonal path-finding and neuronal survival.

The importance of nerve growth factor (NGF) was identified decades ago when NGF-producing cells were grafted to the lesion of an adult rat spinal cord and were shown to facilitate the growth of sensory and noradrenergic neurites. In this pioneering study, a partial sprouting of local motor neurites was observed to be elicited in the injured spinal cord [17]. Another similar approach was conducted by grafting genetically modified Fisher 344 rat primary fibroblast to the injured spinal cords at T7 level of young adult female Fischer 344 strain rats. Genetically modified fibroblast cells produced NGF which induced robust neural ingrowth after grafting to the spinal cord [18]. Notably,

it was also reported that NGF was able to mediate axonal growth following acute and chronic SCI [19].

Neurotrophin-3 (NT-3) is a neurotrophic factor which helps to support the survival and differentiation of existing neurons and encourages the growth and differentiation of new neurons and synapses. Grill *et. al.* reported that primary rat fibroblasts that were genetically modified to produce NT-3 promoted significant partial functional recovery and markedly increased corticospinal axon growth when grafted to acute spinal cord lesion cavities [20]. Another approach indicated that NT-3 infusion was capable of enhancing propriospinal axonal regeneration [21].In this study, both brain-derived neurotrophic factor (BDNF) and NT-3 were delivered simultaneously into rat spinal cord by Alzet minipump. Significantly, more myelinated nerve fibers were observed in the spinal cord with BDNF and NT-3 delivery. This demonstrated that BDNF and NT-3 infusion enhanced propriospinal axonal and axonal regeneration.

Neurotrophin-4/5 (NT-4/5) is a neurotrophic factor that signals predominantly through the TrkB receptor tyrosine kinase. Motor axons, coerulospinal, reticulospinal, and propriospinal axons were reported to respond to NT-4/5 following SCI by significantly increasing axonal penetration into modified fibroblasts grafts, secreting NT-4/5 [22]. However, functional recovery was not observed in this approach. In another study, the growth of regenerating axons in peripheral nervous system was measured in various NT-4/5 level. It demonstrated that the NT-4/5 was able to significantly promote the axons regeneration in peripheral nervous system [23].

BDNF is a prosurvival factor induced by cortical neurons that is necessary for the survival of striatal neurons in brain [24]. To study the capability of BDNF stimulated supraspinal axons regeneration, Menei *et. al.* genetically modified Schwann cells to secrete human BDNF and grafted

these cells into the adult rat spinal cord transection at T8 [25]. The study demonstrated that the concentration of BDNF was increased by the transplanted Schwann cells which improved regenerative responses compared to normal Schwann cells. Another interesting approach was that BDNF was demonstrated to be able to facilitate both central nerve system populations survival and prevention of neuronal atrophy [26]. This study also demonstrated that NT-3 was capable of enhancing the survival of central nerve system population.

Ciliary neurotrophic factor (CNTF) was reported to promote neurotransmitter synthesis and neurite outgrowth in certain neural populations including astrocytes [27]. Talbott *et. al.* demonstrated that CNTF had potential to promote survival and differentiation of oligodendrocytes precursor cells in adult rat spinal cord *in vitro* [28]. Another approach demonstrated that CNTF, released by glial cells, showed very powerful stimulus for optic fiber regeneration after optic nerve crush [29]. In that study, long-distance regeneration of severed optic axons were induced by CNTF after 8 weeks of cell release and the regenerated axons stayed for at least 6 months in the damaged optic nerve.

2.1.2.3 Bridging

The cellular bridging theory was one of the earliest concepts came out in the field of SCI repair. It employed a 'bridge' which was built across the injured area of the spinal cord with permissive cells or materials providing a route for regenerating axons to grow across, allowing for the identification of desired targets, formation of connections, and restoration of neural functions. Thus, a more effective approach to repair SCI might be the combination of neurotrophic factors and bridging method which could lead to long term improvements following SCI [30].

A pioneering study in this field was conducted by Peter Richardson *et. al.* In their studies, Schwann cells were grafted into the injured part of young adult Sprague-Dawley rat spinal cord. One to four months later, many myelinated and unmyelinated axons were observed to be ensheathed by

Schwann cells [31]. This study suggested a tremendous potential of bridging method to repair SCI. However, the study also revealed the problem of the bridging concept including axons indeed regenerated and grew into the grafts, but these axons could not grow out of the graft and re-enter the target tissue of central nerve system. After decades of studies, there are two major issues believed to be important for bridging SCI [30]:

a. A perfect permissive environment is needed to ensure axons to grow through the bridge.

b. A sharp cellular boundary of astrocytes is needed to be formed for axons' off-ramp.

The above mentioned issues are crucial to ensure the axons could be regenerated into the grafts and grow across the bridge as well as reach the target neurons.

Therefore, to construct the bridge, it is important to find a permissive environment which can integrate seamlessly into spinal cord tissue and not stimulate a glial scar reaction while promote axon growth. Besides, axons should be promoted to extend out of the permissive and reach target tissues, rather than being stalled inside the permissive regions. A vast amount of cell types have been studied and grafted into injured spinal cords to create permissive environment, but it is still needed to develop a cell environment containing all these properties. One of the most successful attempts among them was reported by Stephen Davies *et. al.* who identified a specific type of immature astrocyte as permissive to provide successful bridging condition [32]. In that study, it was observed that transplantation of astrocytes promoted robust axon growth and restoration of locomotor functions after acute transection injuries of the adult rat spinal cord.

Another promising idea was to use embryonic central nervous system (CNS) tissue and embryonic astrocytes as bridge permissive to repair SCI. This assumption was based on the property that axons could grow in the embryonic CNS. Several studies demonstrated that the axons were regenerated and expanded into these transplants, but they hardly grow through these transplants. The

host axons can connect to graft neurons in the grafted embryonic CNS, which in turn can send their axons back into the host cord, the grafts acting as relays [30].

As it was introduced previously, the bridging method was often combined with the delivery of the neurotrophic factors because the bridging cells could release neurotrophic factors after genetic modification and the neurotrophic factors facilitated the result of bridging approaches. For instance, it was reported that BDNF was expressed effectively and steadily after genetically modified into Schwann cells. When bridged as a scaffold, these cells were confirmed to be able to promote axons regeneration, including those from brainstem neurons [33]. Blits *et.al.* reported that Schwann cells were able to promote the regeneration of corticospinal axons after modification by NT-3, and positive result was observed in 3 months after grafting [33].

2.1.3 Cell Recognition Motifs

2.1.3.1 Proteins

Over decades, scientists working in the fields of engineering, chemistry, physics, biology biochemistry and medicine have been trying to functionalize polymers to achieve specific cell interaction. At first, they attempted to coat materials with cell adhesive proteins such as fibronectin, collagen and laminin [34]. However, some difficulties were observed during the practice of coating proteins on polymers in view of medical applications. Since proteins had to be isolated and purified, they might elicit undesirable immune responses which were always one of the major problems [34]. In addition, it was impossible for these materials to be employed in long-term applications because of proteolytic degradation [34]. Moreover, only a part of these proteins were able to realize proper cell adhesion due to the random surface orientation issue. Charge, wettability, and topography determined the texture of surface and influenced the conformation as well as the orientation of protein [34]. Protein contains hydrophobic amino acid side chains, which cause significant interaction with

hydrophobic surfaces. Sometimes this leads to protein denaturation or a different presentation of cell binding motifs [34].

2.1.3.2 Peptides

Considering the above problems, small peptides, with cell recognition properties, showed their remarkable efficiency. Compared to proteins, they are more stable under sterilization conditions, heat treatment and pH-variation, storage and conformational shifting as well as easier characterization and cost effectiveness [34]. Since peptides are usually small molecules, they need less space which means they could be planted in higher density [35]. In addition, small peptides usually give only one single cell recognition motif, compared to several different cell recognition motives for proteins. Therefore, a particular type of cell adhesion receptor could be selectively addressed [34].

2.1.3.3 RGD Sequence Related Cell Adhesion Stimulation

Peptide sequence Arg-Gly-Asp (RGD) is, so far, the most popular and widely used peptide sequence to stimulate cell adhesion and promote cell survival on synthetic materials. The fame came from its unique properties, including the widespread distribution (this sequence has been found in large amount of proteins), reasonable availability (this short peptide is easy to be synthesized), and its biological function on cell anchoring behavior and cell survival [34].

Pierschbacher *et. al.* discovered the tripeptide motif RGD as a minimal essential fibronectin based cell adhesion peptide when the authors were trying to reduce large molecule ligands to small recognition sequences [36]. In addition, cell adhesive RGD sites were found in many other extracellular matrix (ECM) proteins, including vitronectin, fibrinogen, collagen, etc. [34].

There are four different overlapping events involved in cell adhesion, which are cell attachment, cell spreading, organization of actin cytoskeleton, and formation of focal adhesions. This whole process is mediated by integrin [37]. At first, gentle shear force is generated when the cell contacts the

surface and ligand binding occurs. Then, the cell body starts to flatten itself and its bottom plasma membrane begins to spread over. Thirdly, actin organizes into microfilament bundles, which becomes stress fibers later on. At last, focal adhesion starts to be generated and it links the ECM and actin cytoskeleton [38-41]. During the four steps cell adhesion process, integrins realize their functions by facilitating physical anchoring and signal transduction through the cell membrane. The integrin signal transmission could be differentiated into two directions: inside-out signaling and outside-in signaling. For inside-out signals, the extracellular binding activities of integrins are regulated by signal from inside, while the other signal is elicited by ECM and transmitted into cells [34].

2.2 Photo-triggers and Photo-caging Strategies

2.2.1 Introduction

For years, biochemical scientists and engineers have been studying in two opposite directions, deep fundamental principles as well as practical applications; however, both of them are targeting the same goal: 'we need not only a functional compound but also tools making the functional activity controllable' [2] . Compounds can make more contribution to researches if they are combined with an effective controller. With the assistance of a controller, more sophisticated experiment could be designed with easier troubleshooting options [2, 42].

2.2.2 Basic Theories and Common Photo-triggers

The desire for an external trigger was increased with the necessity of a controller. After years of developments, light has been used as an external trigger because its high selectivity and harmless to living things if applied correctly [2].

Depending on the unique properties of light, large amount of photo-sensitive compounds were discovered and many photo-caging theories and applications were invented in the past decades.

The first clear attempt in this field was made by Hoffman *et. al.* when they were trying to study

the Na/K pump by preparing a photo-activable adenosine 5′-triphosphate (ATP) [2, 43]. Their study indicated that caged ATP could be incorporated into red blood cells under the condition that the cells were depleted of internal energy stores and the Na/K pump was unable to use this caged ATP as an energy source. After the photo-activation, caged ATP was activated and the pump was re-initiated. This was a proof for the assumption that Na/K pump was K-dependent. In addition, the caged ATP was believed to be an intracellular unmetabolizable and photo-activable energy resource.

There were many interchangeable terms used to demonstrate this photo-caging theory, such as photo-trigger and light-trigger, which sometimes confuses the article search. But the basic theories and understanding of all these words were same, which was to use some photolabile compounds to make a temporary and photo-removable cage to shield the compound function [2].

After decades of development especially past few years, the requests for photo-caging groups have been progressed significantly. Based on several original photolabile compounds, large amount of derivative compounds have been discovered for almost all kinds of specific applications. Meanwhile, a series of indicators have been defined and applied to characterize the property of the caging groups as follows:

- ✓ Extinction coefficient ε (epsilon) was borrowed from physics to demonstrate the efficiency of photo-activation.
- ✓ Based on ε (epsilon), uncaging quantum yield ϕ (phi) was defined to describe the percentage of uncaging reaction happened.
- ✓ The caged compounds (after linked to target molecules) should be soluble and stable in normal vitro and vivo condition without photo trigger.
- ✓ The speed of uncaging reaction should be controllable and the pathway of this reaction should be stable and harmless.
- ✓ Byproduct is allowable but they shouldn’t disturb the photo-uncaging reaction and easily-removable.

- ✓ The wavelength of light used for uncaging should be selective to choose different photo-trigger for different tasks.

Considering the requirement above, some of the most widely used caging groups were collected and listed in Table 1. It was impossible to list all of them, together with a citation of application as well as classification of structure and caging-uncaging theories. The caging groups were divided into two classes (2-nitrobenzyl derivatives and coumarin-4-ylmethyl derivatives), each of them possessed advantages and disadvantages, which made them suitable for various kinds of caging applications.

Table 1. List of some common photo-caging compounds used in the study

Derivatives	Full Chemical Name	Chemical Structure
2-Nitrobynzene Derivatives	R=H, 1-ethyl-2-nitrobenzene group R=Me, 1-isopropyl-2-nitrobenzene group [43-45]	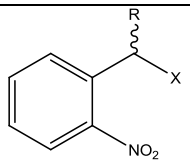
	R=H, 1-ethyl-4,5-dimethoxy-2-nitrobenzene R=Me, 1-isopropyl-4,5-dimethoxy-2-nitrobenzene group [46, 47] [48, 49]	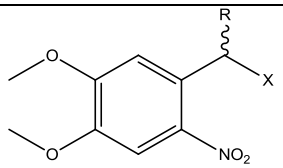
	ANP[50] 2-amino-2-(2-nitrophenyl)acetic acid	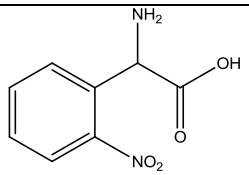
Coumarin-4-ylmethyl Photo-triggers	R=H, 6-bromo-4-ethyl-7-hydroxy-2H-chromen-2-one R=CH_3CO,6-bromo-4-ethyl-2-oxo-2H-chromen-7-yl acetate [46]	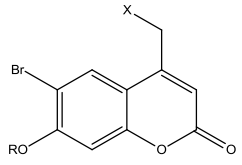

	R=Me, 7-(dimethylamino)-4-ethyl-2H-chromen-2-one R=Et, 7-(diethylamino)-4-ethyl-2H-chromen-2-one [46] [51] [52]	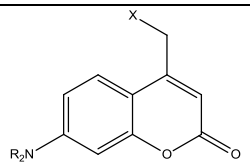
	4-ethyl-7,8-dimethoxy-2H-chromen-2-one [52]	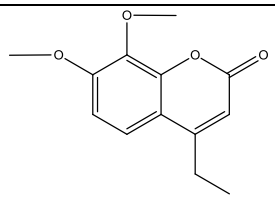
	R=H, 4-ethyl-7-hydroxy-2H-chromen-2-one R=CH_3, 4-ethyl-7-methoxy-2H-chromen-2-one R= CH_2 COOH, 2-(4-ethyl-2-oxo-2H-chromen-7-yloxy)acetic acid [53-59]	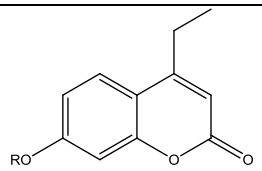

2.2.3 2-Nitrobenzyl Derivatives

2.2.3.1 Mechanism of Uncaging Reaction

2-nitrobenzyl derivatives were the first series of compounds applied in photo-caging applications. After decades of development, its derivatives and their caging strategies for different materials were relatively mature. The mechanism of the photo-uncaging reaction was studied and promising results were obtained. Wirz *et. al.* published the photo-uncaging reaction mechanism of 2-nitrobenzyl compounds (Figure 2a) which further demonstrated the photo-uncaging reaction of 2-nitrobenzyl compounds [60, 61].

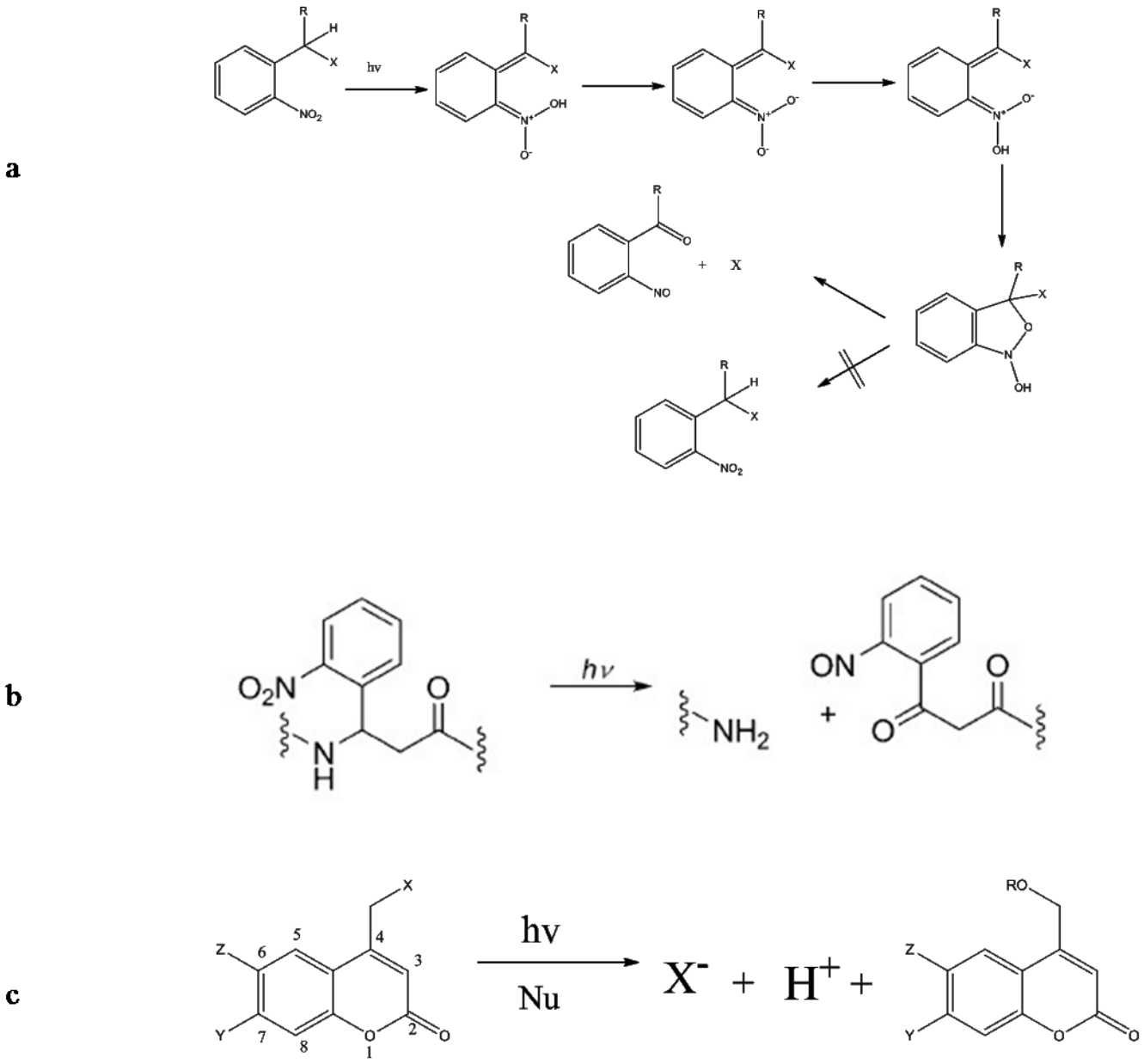

Figure 2. Schematic diagrams showing activation reactions for various caging groups. (a) Photo-uncaging mechanism of 2-nitrobenzyl compounds; (b) Photo-reaction diagram of Anp linker; (c) Photo-reaction diagram of coumarin. (hv represents photon energy and Nu represents nucleophilic molecules.)

2.2.3.2 Target Molecules and Caging Strategies

2.2.3.2.1Caging ATP

ATP was the first compound applied to this 2-nitrobenzyl theory. It was accomplished by Hoffman *et. al.* when they were trying to study the Na/K pump [43]. In this study, they successfully caged the phosphate group of ATP by a derivative 1-(2-nitrophenyl) ethyl group in 2-nitrobenzyl family. After the first attempt, the method of caging ATP was frequently used and gradually developed to be a method in researches from other fields. Even in recent years, caged ATP, with various photo-trigger derivatives, was still playing an irreplaceable role in biochemical researches. Ito *et. al.* applied a photo-responsive adenosine triphosphate (azo-ATP) *in vitro*. In their study, azo-ATP was used to replace normal ATP in order to demonstrate that their compound was a suitable substrate for T7 ribonucleic acid (RNA) polymerase and the resulting RNA served as a template for reverse transcription [62]. For caging ATP study, 1-(2-nitrophenyl) ethyl and 2-(2-nitrophenyl) propyl groups were used to study the photo-release of caged ATP [63]. It demonstrated that the decay of the intermediate aci-nitro anion was the rate-determine step of ATP release.

2.2.3.2.2 Caging Nucleotides

Nicotinamide adenine dinucleotide phosphate, abbreviated as NADP or TPN (triphosphopyridine nucleotide), is a coenzyme in anabolic reactions. NADPH is a reducing agent in lipid and nucleic acid synthesis. Therefore, in many bio-chemical studies, it is remarkably necessary to photo-labile cage NADP and realize its controllable release [63]. Extensive studies have been implemented in caging nucleotides by 2-Nitrobenzyl derivatives in various ways. NADP compounds have been caged according to 2-nitrobenzyl chemistry by various groups [63]. These caged NADP derivatives generated long-lived intermediates during the photo-reaction. According to the available data and mechanism analysis, intermediates' lifetime was as long as hundreds seconds (pH 7.3), indicating these compounds were unlikely to be useful in the applications with high time-resolution requirement.

Therefore, further study is still needed to modify product release rate of caged NADP derivatives [63].

2.2.3.2.3 Caging Peptides and Proteins

With the development of biological and tissue engineering, extensive research has been done in caging peptide and protein through specific route and for various certain usages. For example, caging groups and caging strategies were developed aiming to solve crucial problems including limited kinds of functional groups on peptides and the steric hindrance from bulky caging groups [63]. When caging strategies for unnatural amino acid (non-proteinogenic amino acids that either occur naturally or are chemically synthesized) got matured, scientists couldn't even find any inhibition using caged moiety and its location on the protein. Bosques *et. al.* reported that they successfully cleaved the inhibitory unit and initiated fibril formation by activating a nitrobenzyl-type linker, which was planted in the peptide during peptide synthesis procedures [64]. Another remarkable approach was made by Kyle *et. al.* who caged aspartic acid using 2-nitrobenzyl group. In this study, they caged the amino acid, confirmed the photolysis reaction, and studied the neuron reaction to both caged and uncaged amino acid. The authors demonstrated that bioactivity of aspartic acid was caged by 2-nitrobenzyl group could be regained by UV irradiation [65]. A further approach, implemented by Goubko *et. al.*, demonstrated that the bioactivity of peptide sequence RGDS could be caged by 2-nitrobenzyl group. Regarding cell studies *in vitro*, it indicated that the biological activity of the peptide was caged when the side chain amide of glycine was caged by 2-nitrobenzyl group, which was regained by UV irradiation [66]. In addition, this was the only caging position to get acceptable stability and caging yield.

2.2.3.2.4 Anp Linker

A series of recently approaches about 2-nitrobenzyl derivatives caging peptides was implemented by 3-amino-3-(2-nitrophenyl) propionyl linker (Anp linker), with the advantages of high liberation

yield and shorter photolytic half-life [67]. Anp linker was recently reported to be used on preparing photolabile cyclic-caged peptide according Solid Phase Peptide Synthesis (SPPS) (detailed introduction about SPPS will come at chapter 2.4). The photo-activity of the caged compound has been confirmed and the photo-uncaging reaction was also reported (shown in Figure 2 (b)) [50]. Similar to other photo-active 2-nitrobenzyl derivatives, its caged carboxyl groups were released with amide terminus.

2.2.3.2.5 Caging Fluorophores

Fluorophores are fluorescent compounds that can re-emit light upon light excitation which plays a crucial role in various researches. They would contribute significantly if fluorescent properties of fluorophores could be controlled. The general strategy of caging fluorophores was to disturb or even change the electronic structure of whole molecule by binding caging groups onto the fluorophores. In this way, the fluorescent property of the fluorophore could be temporarily attenuated or even sheltered until it is activated by specific kind of UV irradiation [63].

2.2.4 Coumarin-4-ylmethyl Photo-triggers

2.2.4.1 Introduction

Coumarin, in the benzopyrone chemical class, is a fragrant organic chemical compound which is a colorless crystalline substance in its standard state. Coumarin was naturally found in large amount of plants, especially high concentration in the tonka bean (Dipteryx odorata), Vanilla grass (Anthoxanthum odoratum), sweet woodruff (Galium odoratum), mullein (Verbascum spp.), sweet grass (Hierochloe odorata), cassia cinnamon (Cinnamomum aromaticum), melilot (Melilotus spp.), deers tongue (Panicum clandestinum) and sweet clover (Fabaceae spp.). The name, coumarin, came from a French word, coumarou, for the tonka bean. Coumarin has a sweet odor and has been used in perfumes since 1882. When it was found to be in high concentrations in forage plants, coumarin was

used as a bitter-tasting appetite suppressant, and has been produced by plants as a defense chemical to discourage predation [68].

The lately developed Coumarin-4-ylmethyl family photo-triggers were mainly used to cage carboxylates phosphates amines alcohols phenols and carbonyl compounds. However, the applications of coumarin photo-triggers in proteins and peptides have not been extensively reported. Coumarin is the parent compound of the chromophore which was highlighted in Figure 2 (c). It could be realized as a member of arylalkyl-type photo-removable protecting groups [69]. During the photolysis reaction, an anion of the leaving group is produced by the cleavage of C-heteroatom bond (mostly oxygen) between C-4 methylene and X (leaving groups) and a dissolved coumarin is generated as a photo by-product.

Studies of coumarin had been mainly focused on the utilization of their fluorescent properties like fluorogenic enzyme substrates, fluorescent labeling agents and laser dyes [63]. The photosensitivity of (coumarin-4-yl) methanol was first discovered by Givens *et. al.* from a phosphate ester about 30 years ago [70]. With a yield of 0.038, a benzene solution of (methoxycoumarin-4-yl) methyl ester of diethylphosphate was photolyzed. The study also clarified its usage as a fluorescent labeling compound for nucleophilic molecule (Nu) and suggested the generation of an electrophilic coumarin-4-ylmethyl cation upon photolysis. Coumarin photo−triggers were grouped into four categories based on their structure similarity (Table 1). Photochemical, photophysical and physical properties of coumarin-caged compounds were usually determined by the structure of bonded molecules [42].

2.2.4.2 Target Molecules

2.2.4.2.1Phosphates

Caging phosphates was the most successful application for coumarin-based photo-triggers. ATP was successfully caged by (7-(diethylamino)coumarin-4-yl) methyl at the phosphate group and

utilized in the light-control *in vitro* transcription [71]. It was also reported that the synthesized 6-bromo-4-diazomethyl-7-hydroxycoumarin (Bhc-diazo) could cage messenger RNA (mRNA) when binding to its sugar-phosphate backbone [72]. The study indicated that the translation activity of the mRNA was dramatically decreased after it was caged and the activity was regained when the caged mRNA was activated by long-wave UV exposure (350 to 365 nm).

2.2.4.2.2 Sulphates and Carboxylate

Photochemistry analysis of Coumarin-4-ylmethyl carboxylates and sulfates esters showed similar result to phosphate esters. Only a few caged compounds have been reported so far due to low photo-efficiencies of the coumarin-4-ylmethyl (MCM) group esters of simple aliphatic acid. MCM ester of heptanoic acid's (MCM-OHep) photolysis quantum yield was reported to be 0.0043, which was smaller than that of MCM-phosphates for more than one order of magnitude [63].

2.2.4.2.3 Alcohols and Phenol

Coumarin-4-ylmethyl photo trigger caged carbonates can release parent alcohols or phenols under UV irradiation. The same leaving group was detected for all four types of coumarin-caged carbonates synthesized. Based on the chemical and physical properties of the studied compounds, the 6-bromo-7-hydroxycoumarin group was used as photo-trigger for hydroxyl-containing molecules such as sugars, amino acids and lipid mediators [42].

2.3 Hydrogels

2.3.1 Introduction

Hydrogels are cross-linked polymer chains that are hydrophilic with water dispersion medium.

Hydrogel, cross-linked poly (2-hydroxyethyl methacrylate), was first used as a soft contact lens material [73]. Chemical structure of cross-linked poly (2-hydroxyethyl methacrylate) was given in Figure 3. According to the definition of hydrogels given by Peppas, hydrogels were water-swollen, cross-linked polymeric structures containing: (1) covalent bonds produced by the reaction of one or more comonomers; (2) physical cross-linked due to chain entanglements; (3) association bonds including hydrogen bonds or strong van der Waals interaction between chains; or (4) crystallites bringing together two or more macromolecular chains [74].

Depending on various parameters, hydrogels were differentiated into various categories based on the preparation method, overall charge, and structural and mechanical characteristics.

For the capability of retaining large amount of water and their softness as well as rubbery consistence, hydrogels were extraordinarily suitable for numerous applications in the fields of pharmaceutical and medical industry. Thanks to their highly water content, hydrogels also possess flexible degree, which is extraordinary similar to natural tissue [74].

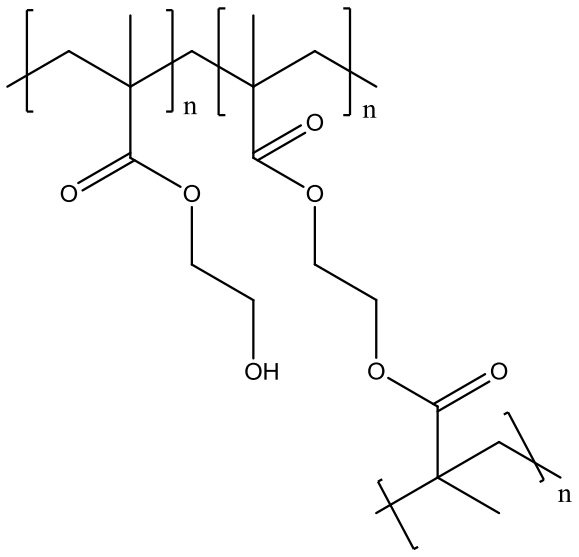

Figure 3. Chemical structure of cross-linked poly (2-hydroxyethyl methacrylate)

2.3.2 Biopolymer-based Hydrogel Systems

2.3.2.1 Polysaccharide Hydrogels

2.3.2.1.1 Agarose

Agarose is purified from marine algae and it is a linear galactan hydrocolloid [75]. The special properties of agarose are temperature dependent phase state and gelation, totally melting in 95℃ and gelation between 32℃ and 45℃ [76]. This unique state of temperature dependent property gave agarose a special application, injectable models, with the assistant of liquid nitrogen to cooling down [77]. Remarkably, agarose gel electrophoresis was shown to be the most effective way to separate deoxyribonucleic acid (DNA) fragments with size variation from 100bp to 25 kb. Since the phosphate backbone of the DNA is usually negatively charged and it has a uniform mass/charge ratio, when placed in an electric field, DNA fragments move to the positively charged anode and the distance they travel is proportional to the log of its molecular weight. Therefore, DNA fragments are separated by various sizes [78].

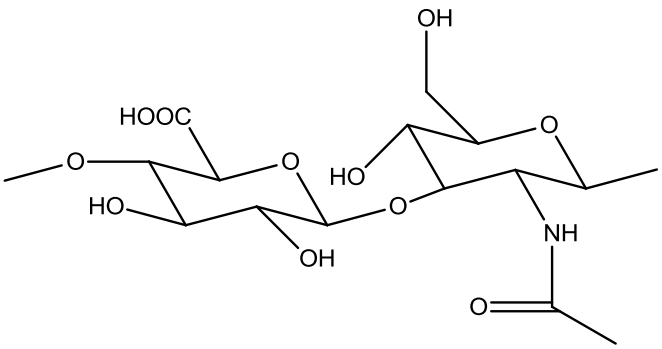

Figure 4. Chemical structure of hyaluronic acid

2.3.2.1.2 Hyaluronic Acid

Hyaluronic acid (HA) is a nonsulphated glycosaminoglycan which is formed by alternated D-glucuronic acid and D-N-acetylglucosammine units. Alternated β-1, 4 and β-1, 3 glycosidic bonds are applied to link these units together (Figure 4) [79, 80]. HA was famous for its applications in cartilage, vitreous humor and ECM of skin [74]. In the 1970s, HA was firstly reported as a biomedical product (Healon), which was approved by Food and Drug Administration (FDA) for the usage in eye surgery (corneal transplantation) [81]. At present, the most commonly used HA-based product in market is HYAFF (benzyl ester of HA) [74]. HYAFF products existed in several degrees with different mechanical properties and biological responses, which have already been reported by several research groups. However, in research area, the polymerization of methacrylate-functionalized HA is still a widely used HA chemically cross-linking strategy [74]. To realize the endothelial cell attachment within microfluidic channels for blood vessel formation, HA was combined with collagen and formed semi-interpenetrating networks (semi-IPNs). The encapsulation and subsequent proliferation of fibroblast and chondrocyte on semi-IPNs were also reported [74]. Combined with alginate and poly-L-lysine, HA was used to develop scaffolds for several tissue engineering applications including nerve regeneration [82-85]. Horn *et. al.* used Michael's addition to combine HA with acrylate-functionalized polyethylene glycol (PEG) thiol-modification to form a hydrogel which was suitable for SCI repair [86]. Modified by RGDS peptide sequences, HA hydrogel provided a suitable condition for cell attachment [66, 87-89]. It is worth mentioning that, RGD peptides were bonded to test its bioactivities with live cells *in vitro* with cross-linker adipic acid dihydrazide (ADH) and coupling reagent 1-Ethyl-3-(3-dimethylaminopropyl) carbodiimide (EDC) [66, 90]. In these

researches, part of the carboxyl groups were activated by EDC for ADH cross-linking while others were preserved for peptide bonding as shown in Figure 5. Recently, matrix metalloproteinase (MMP)-sensitive HA-based scaffolds were reported to adjust the degradation speed for new tissue formation. Generally, cross-linkers, possessing MMP-cleavable peptides, were selected to imitate the remodeling characteristics of natural extracellular matrices by cell-derived MMPs [91]. Finally, combined with stem cells, HA was also applied as injectable material for tissue growing purposes [92].

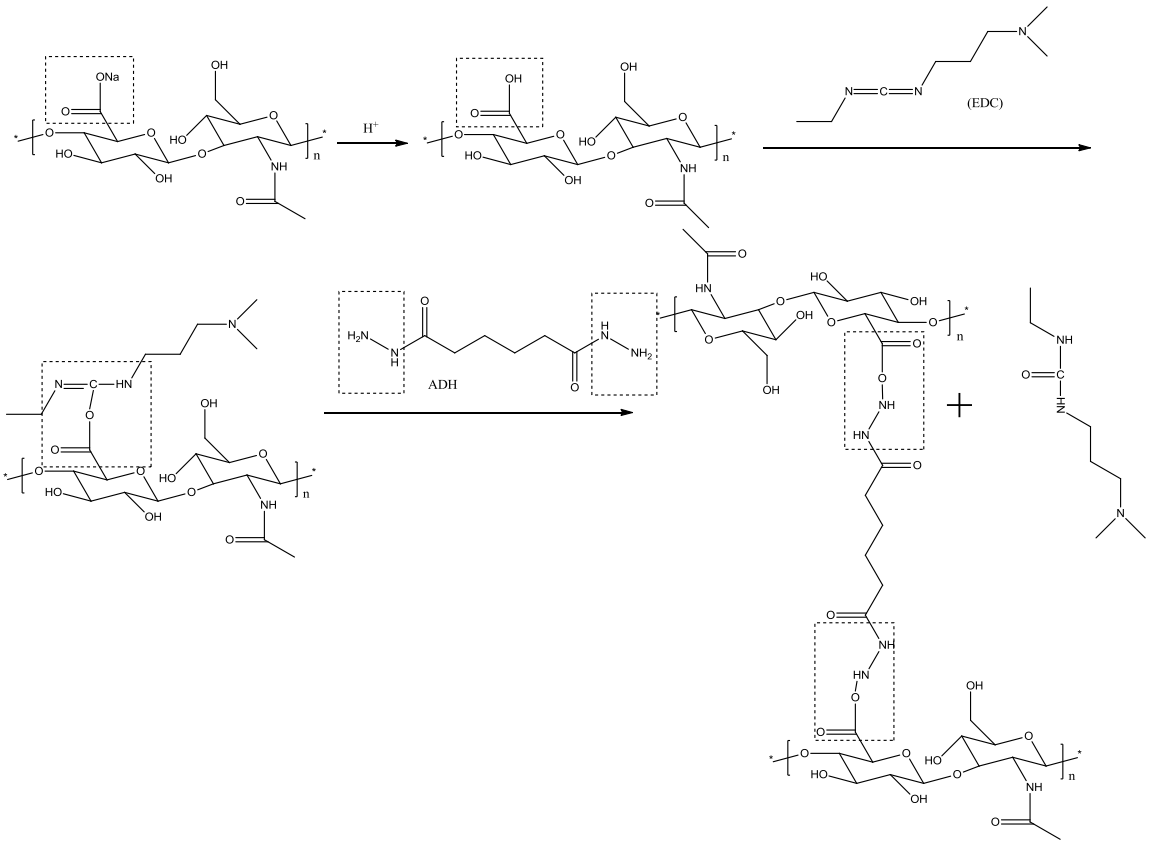

Figure 5. Schematic diagram showing mechanism of HA-ADH cross-linking

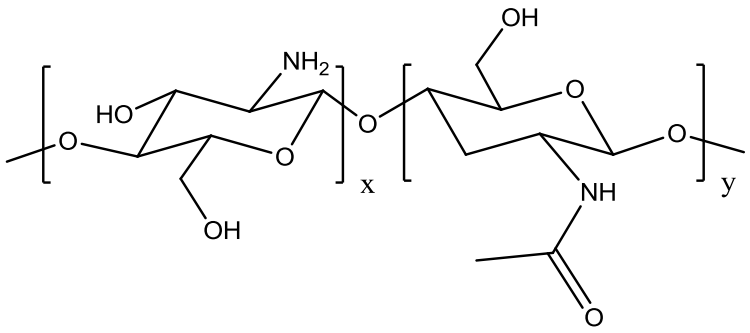

Figure 6. Chemical structure of chitin

2.3.2.1.3 Chitosan

Chitosan, obtained from the shells of crabs and shrimp, is a partial deacetylated derivative of chitin (Figure 6). Chitosan is a biocompatible, cationic polymer with good water solubility at pH up to 6.2. The dissolution of chitosan could be transferred from pH-responsiveness to thermo-responsive system by addition of polyol salts like β-glycerophosphate (GP). Gelation occurs when it's heated to body temperature. Chitosan is stable at room temperature and its gelation time is increased with its deacetylation level decreasing [74].

Induced by the hydration of chitosan chain, chitosan solubility at pH 7 and room temperature could be promoted by GP. After heated to body temperature, the bound water of chitosan is released which leads to the chain interactions and subsequent gelation. Interactions involved in the gelation process are as follows [74]: (1)Electrostatic attractions ammonium groups on chitosan and phosphate group on GP. (2)Hydrogen bonding between chitosan chains. (3)Hydrophobic interactions between chitosan molecules.

The scaffold application of chitosan in tissue engineering was also studied. It showed that cortical cell survival was improved if the modification was not more than 0.1%, or the outgrowth was hindered significantly. A common application for cross-linking chitosan-based scaffolds was the use of glutaraldehyde [74]. The gelation rate for this was increased by increasing the concentration of either chitosan or glutaraldehyde [93].

2.3.2.1.4 Cellulose Derivatives

Cellulose, with the molecular formula $(C_6H_{10}O_5)_n$, is a linear polymer chain, possessing hundreds

to over ten thousand of β(1→4) linked D-glucose units [94]. It is the main structural component of cell wall of green plants. In 1838, Cellulose was first extracted from plant, studied, and reported by a French chemist Anselme Payen [95]. He was named the 'Father of Cellulose Chemistry' for his contributions in cellulose research.

There were much more remarkable properties of cellulose derivatives have been discovered. The gelation of several cellulose derivatives was generated upon heating. Moreover, combined with hydroxyapatite, cellulose revealed a great potential in the applications of bone tissue engineering [74].

2.3.2.1.5 Alginate

Alginate, also called as align or alginic acid, is widely distributed in the cell walls of brown algae. Binding with water, it is able to absorb 200-300 times of its own weight of water and forms a viscous gum. Alginic acid is a linear copolymer composed with β-D-mannuronate and α-L-glucuronate unites. Coupled with RGD peptides or growth factors, alginate was applied in cell-interactive applications. Moreover, combined with calcium phosphates, it was also suitable in bone tissue engineering applications [74]. Another remarkable application of alginate hydrogel was the use of alginate hydrogel as vehicle for drug delivery. It has been reported that daunomycin was used as a model for low molecular weight drugs to study the property of alginate as a drug delivery vehicle [96]. In that study, daunomycin was bonded to alginate hydrogel by labile covalent bond. After the covalent linkage between the drug and the polymer was hydrolyzed, the daunomycin was released. It demonstrated that drug could be released in a wide range of release profiles (from 2 days to 6 weeks) and the biological activity of the released daunomycin was preserved.

2.3.2.2 Protein Hydrogels

2.3.2.2.1 Collagen

Collagen is a major ECM protein existing in various tissues. It has a very special secondary structure called collagen helix, or type-2 helix. This structure consists a triple helix made of the repetitious amino acid sequence glycine-X-Y, where Z and Y are frequently proline or hydroxyproline [97]. Generally, lyophilisation techniques or stereo lithography methods were implemented to produce the porous collagen-based scaffolds. In addition, 3D collagen matrices were built by recently developed cryogenic direct-plotting system [74]. With the assistance of the 3D collagen matrices, 3D collagen scaffolds were designed and made great contribution to the study of cancer. In this way, the invasive character of cancer cells and the interaction between cancer cells and other cell types were particularly analyzed in 3D environment [98]. Another recently published approach demonstrated that moderately cross-linked collagen scaffolds was used as heart valve in tissue engineering, which possessed the advantages of immediately function arouse, cell infiltration tolerant and gradual remodeling [99].

2.3.2.2.2 Fibrin

Fibrin (exists in clotting of blood) is non-globular, fibrous protein which is also called factor Ia. Over a wound site, it is polymerized to form a ‘mesh’ that becomes a hemostatic plug or clot [100]. In recent years, fibrin glue was invented and used clinically as an adjunct therapy to stem bleeding. In 2007, Santoro *et. al.* reported that fibrin glue was used, instead of sutures or staples, to enhance healing and minimize scarring [101]. In the deep brain stimulation treatment of Parkinson’s disease,

fibrin glue was used as a protective stabilize layer between the dura and methyl methacrylate bioglue [101]. When used for drug delivery, it was reported that fibrin retained the capacity of vascular endothelial cell growth factor (VEGF) to support endothelial cell proliferation when VEGF was bonded to fibrin [102].

2.4 Solid Phase Peptide Synthesis

Peptide normally refers to amino acid chains with little secondary structure. In organic chemistry, peptide synthesis is to link amino acids via peptide bonds, also called amide bonds. During the synthesis, carboxyl group (C-terminus of the amino acid) and amino group (N-terminus of the amino acid) are coupled.

Although people have been able to link amino acids together and form peptide bonds for over a century, the first artificial synthesized peptide, including oxytocin and insulin, was available around 60 years ago. It demonstrated how difficult it was to chemically synthesis a chain of amino acids [103].

Solid-phase peptide synthesis (SPPS) was invented by Robert Bruce Merrifield [104], which eventually leaded to a paradigm shift in the peptide synthesis community. SPPS is now a generally accepted method for creating peptides and proteins in lab under synthetic manner. This method also makes it possible to synthesis peptides which are difficult to express in bacteria, with unnatural amino acids, and synthesis peptides with D-amino acids.

In brief, the SPPS mechanism is consisted of repeated cycles of coupling-wash-deprotection-wash. It involves coupling of the C-terminus of a N-protected amino acid unit to the free N-terminus of a solid phase attached peptide and deprotection of this unit to reveal a new N-terminus amine for further amino acid attachment (Figure 7). The superiority of this technique

relies on solid phase which could be washed after each step of reaction to remove all the excess reagent, amino acid, and byproduct.

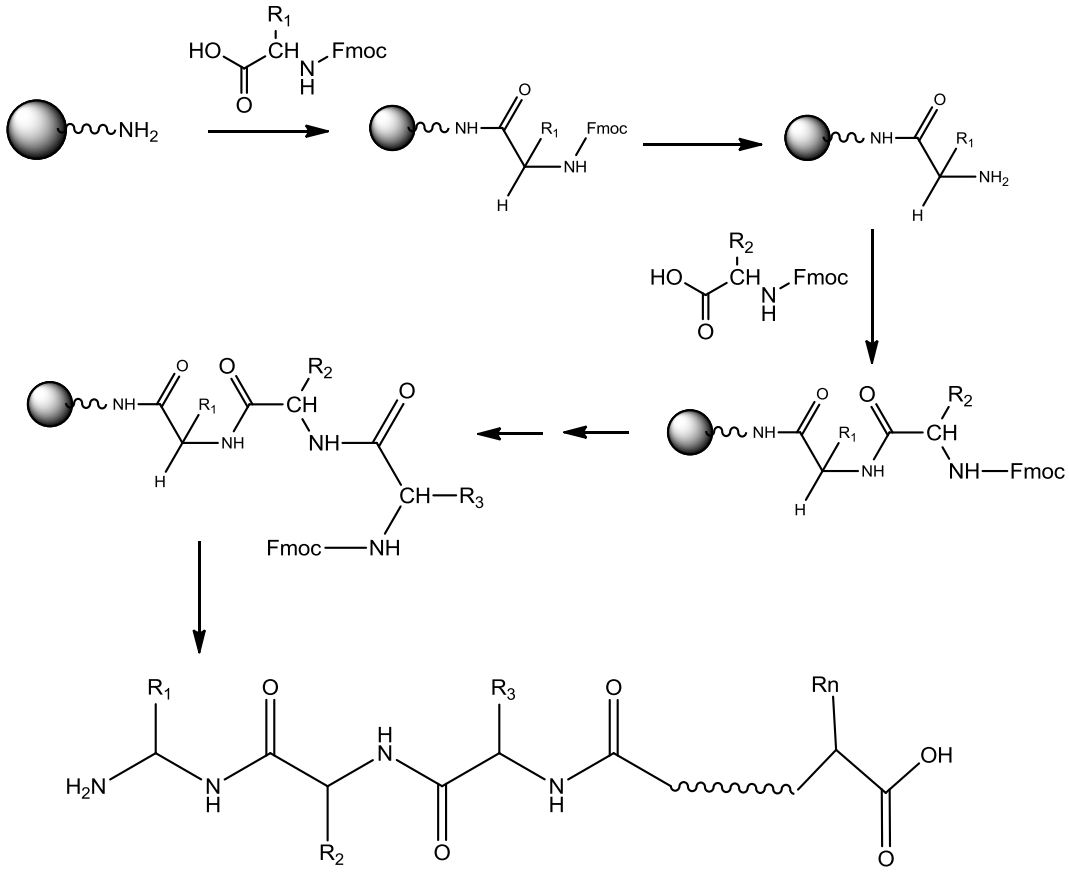

Figure 7. Schematic diagram showing general theory of solid phase peptide synthesis

Once all synthesis cycles are finished, the side-chain protecting groups are still needed to be removed and the peptides are still linked on the solid phase. Trifluoroacetic acid (TFA) could be applied to cleave peptide from solid phase and remove protecting groups meanwhile. Penningtoon *et. al.* reported detail protocols for SPPS in 1994 [105].

2.5 Switchable Surface Cell Patterning

With the developments in the fields of materials and tissue engineering, there were increasing amount of research requests appeared about tissue engineering in micron level. It, on the other hand,

needs the cellular environment to be precisely controlled and manipulated because cells are strongly interacted with surrounding environments like ECMs and other cells. This is so-called cell patterning [106]. Therefore, cell patterning, in particularly surface cell patterning, is mostly depended on the control of cell-surface interactions in micron level [106, 107]. After decades of development, photo-switchable surface techniques have become one of the most extensively used techniques in this field. There were many switchable surface cell patterning strategies relied on the photo-switchable surfaces. For instance, Goubko *et. al.* reported fibroblast pattern by coating synthesized photo-labile caged RGDS peptides on cross-linked HA hydrogel. The cell patterning was clearly observed after the specific position of the photo-switchable HA surfaces were modified by UV irradiation [66]. Another similar approach was made by patterning cells on cyclo[RGD(DMNPB)fK] coated silica surfaces. After the UV irradiation through photo-mask, a remarkable cell patterning graph was also observed [108]. Besides the photo-switchable surfaces, heat-switchable surfaces played a significant role in the field of switchable surface cell patterning. For example, plasma polymerized poly (N-isopropyl acrylamide) was used in cell patterning when modified by addressable microheaters. It was demonstrated that the material surface was switched between adhesive and non−adhesive behaviors as a function of temperature, and the transition of the material could occur spatially under the control of individual heaters [109].

Chapter 3 Hypothesis and Objectives

Hypothesis

The hypothesis of this whole project is, after SCI, a biomaterial (shown in Figure 1) would be planted into the injured part of spinal cord. This material would contain various factors facilitating directed axon growth. Photo-labile caged RGDS peptide is a promising candidate among the most important factors. The caged peptide could be bonded to the whole material providing a non-adhesive 'black background'. Cell adhesive permissive channels with 'active RGDS peptide' could be built by two-photon laser activation inside the material. In these channels, it would be possible for the axons of injured neurons to grow through and reach the target neurons.

Reviewing the methods published to cage RGDS peptide, caging groups were normally bonded with one of the amino acids prior synthesizing peptide chain. These caging methods inevitably faced difficulties caused by caging group. The recently published cyclic caging strategy is promising to overcome these difficulties [50]. To fit RGDS sequence into cyclic caging strategy, the peptide needs to possess following characteristics:

1. The side chain functioning groups of RGDS sequence should be free for receptor binding.

2. Anp linker (available in the market) needs to be planted in this peptide chain to make the peptide photo-cleavable.

3. N-terminus is the best place to locate the anp linker to preserve its photolabile property in synthesizing procedures.

4. The peptide chain should be long enough to be flexible for cyclic caging reaction, which

could be fulfilled by introducing adoa.

5. An extra amino group is required on the side chain of peptide to connect the peptide and biomaterial, for which lysine is one of the best candidate.

Therefore, the peptide sequence was designed to be NH_2-Anp-Arg-Gly-Asp-Ser-Adoa-Lys-COOH.

+

Objectives

1. To prepare cyclic caged RGDS peptide by using cyclic caging strategy and solid phase peptide synthesis method
2. To employ Anp linker to make the caged peptide photo-cleavable.
3. To confirm the accuracy of peptide synthesis by mass spectrum, followed by reversed phase high performance liquid chromatography (RP-HPLC).
4. To confirm peptide stability under various pH conditions by circular dichroism (CD) study; to confirm photolysis activity of the caged peptide by ultraviolet (UV) photolysis study; and to confirm biological activity of caged and uncaged peptide by cell study.

Chapter 4 Experiment

4.1 Materials

For peptide synthesis, protected standard amino acids, Fmoc-Arg(Pbf)-OH, Fmoc-Gly-OH, Fmoc-Asp(OtBu)-OH, Fmoc-Ser(OtBu)-OH, and coupling reagent 2-(1H-benzotriazole-1-yl)-1,1,3,3-tetramethyluronium hexafluorophosphate (HBTU) were purchased from Anaspec (Fremont, CA); Fmoc-8-amino-3,6-dioxaoctanoic acid (Adoa) was purchased from Peptide International (Louisville, KY); 3-Nα-Fmoc-Amino-3-(2-nitrophenyl) propionic acid (Anp linker) was purchased from Advanced Chemtech (Louisville, KY); H-Lys(Boc)-2-ClTrt resin was purchased from Novabiochem (Albuquerque, NM); and tentagel amide resin was purchased from Intavis Bioanalytical Instruments AG (Germany). In addition, 1-Ethyl-3-(3-dimethylaminopropyl) carbodiimide (EDC) was purchased from Fisher Scientific (Ottawa, ON). All other chemicals were obtained from Sigma-Aldrich (Oakville, ON) and used as received unless indicated otherwise.

4.2 Methods

4.2.1 Peptide Synthesis

The synthesis procedures for cyclic-caged RGDS are shown in Figure 8. There are three main steps:

I. A linear peptide *H_2N-Anp-Arg-Gly-Asp-Ser-Adoa-Lys-COOH* was synthesized by Fmoc-SPPS strategy with all the side-chain functional groups protected. In this peptide synthesis step, automatic peptide synthesizer from Intavis Biochem AG (Germiny) was employed to synthesize

the linear peptide. The software defaulted synthesis protocol (2 times deprotection, 2 times coupling, HBTU/DIEA coupling reagent system, and no capping step) was applied to ensure the yield and purity of the resulting peptide. H-Lys(Boc)-2-ClTrt resin, assisted by 1% TFA in dichloromethane (DCM) cleavage system, was used to ensure that peptide product was side-chain protected and had free N and C terminuses [110]. Sample product was purified by two cycles of ice-ether washing followed by lyophilisation. The resulting product was a pure sample as evidenced by a single peak by HPLC analysis. The product of this SPPS step was further confirmed by both electrospray ionization-mass spectrum (ESI-MS) and matrix-assisted laser desorption/ionization mass spectrum (MALDI-MS).

II. The second step for peptide preparation was cyclic-caging reaction by an intra-molecular coupling reaction between the N-terminus and C-terminus of the linear peptide to form a cyclic structure. In a particular reaction, 5 mg of the linear peptide was dissolved into 100 ml solvent (DMF: DCM=1:10), to which 30 mg HBTU and 10 µl N-methylmorpholine (NMM) were used as coupling reagent. The reaction was allowed to proceed overnight at room temperature, after which 1:1 water/ethyl acetate extraction system was used to extract the peptide product. The ethyl acetate layer of the extraction system was preserved and rotary evaporated to obtain raw product. To further purify, the raw product was dissolved in water/acetonitrile (1:1) and freeze-dried to obtain a white fluffy powder product.

III. Subsequently Reagent B (88% TFA, 5% water, 5% phenol, and 2% triisopropylnaphthalenesulfonic acid) was used to remove side-chain protecting groups at room condition for four hours. Finally, the product was washed by ice ether and then freeze-dried to

obtain cyclic-(NH-Anp-Arg-Gly-Asp-Ser-Adoa-Lys-CO) [110]. RP-HPLC was applied for the purification of sample product (more purification detail is shown in discussion part).

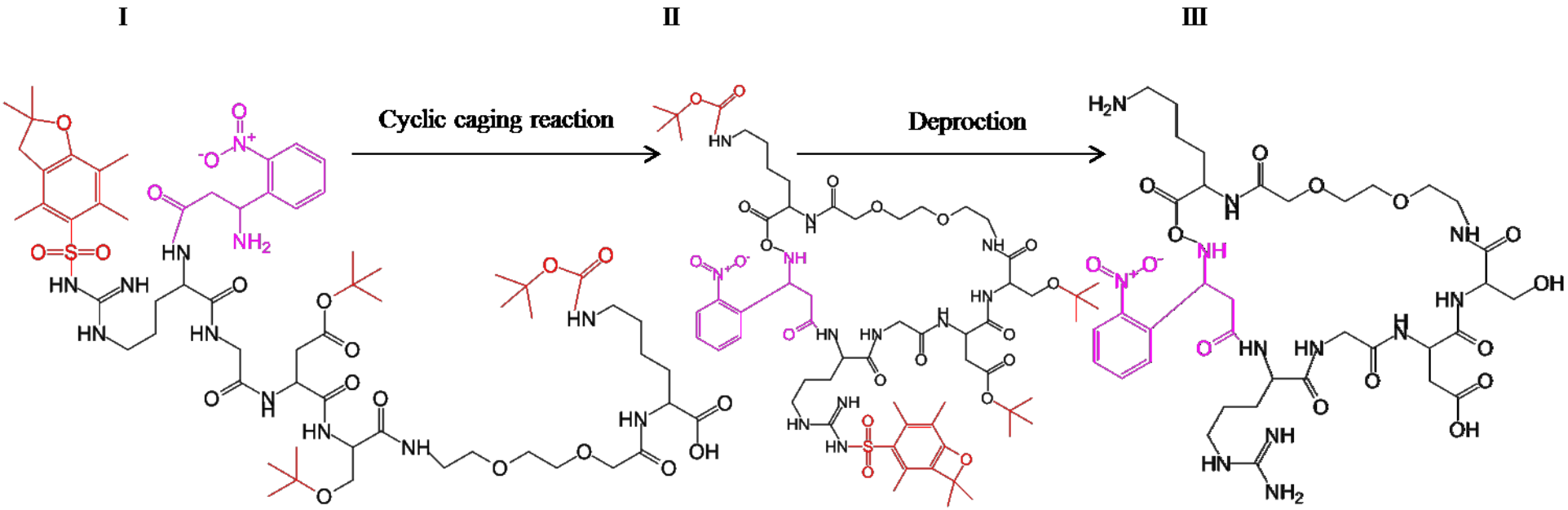

Figure 8 Synthesis procedures for cyclic caged RGDS. Step I is demonstrating SPPS. Step II is demonstrating cyclic caging reaction. Step III is deprotection.

4.2.2 Circular dichroism (CD) spectroscopy

To study the stability of the final caged peptide product at different pH conditions, CD study was carried out. Cyclic caged RGDS peptide (7 mg) as dissolved in dd-water to prepare a 1mg/ml peptide solution that was equally divided into 7 aliquots. 1M HCl or 1M NaOH was used to adjust the pH of each aliquot to 3.51, 4.26, 4.91, 5.85, 6.70, 7.70, and 8.73 separately. A J-810 spectropolarimeter (JASCO, Victoria, BC) was used to obtain CD spectra for each sample at different pH conditions.

4.2.3 Mass Spectrum Analysis

To confirm the chemical structure of the obtained product, ESI-MS (Micro Mass Q Tof Resolution 8000) and MALDI-MS (Bruker MALDI Microflex) were used.

4.2.4 Kinetic Study

To study the kinetics of the photo-uncaging reaction (as shown in Figure 9) of the cyclic caged peptide, near-UV irradiation from a 365 nm long-wave UV Lamp (Black-Ray B-100 Long-wave UV lamp, 100 W, UVP, Upland, CA) was employed. 1 mg/ml caged RGDS peptide solution (200 µl) was made with PBS buffer. This solution was exposed to UV light (10 mW/cm^2). At predetermined time points, 20µl solution was transferred to a pre-labeled tube containing 0.9 ml of water frozen in ice. When reacted solution was transferred, the tube was immediately placed in liquid nitrogen (dark place) to terminate uncaging reaction. When the whole experiment was finished, RP-HPLC (Varian Prostar, with C-18 analytical column) was used to determine the concentration of cyclic caged RGDS

peptide in each sample. Then all the peptide concentration data and corresponding UV exposure time were plotted in a graph ($\ln[A]/[A]_0$ vs. t). Linear fitting was done by OriginLab software (MA, US) to decide the fitness of our data to linear reaction theory.

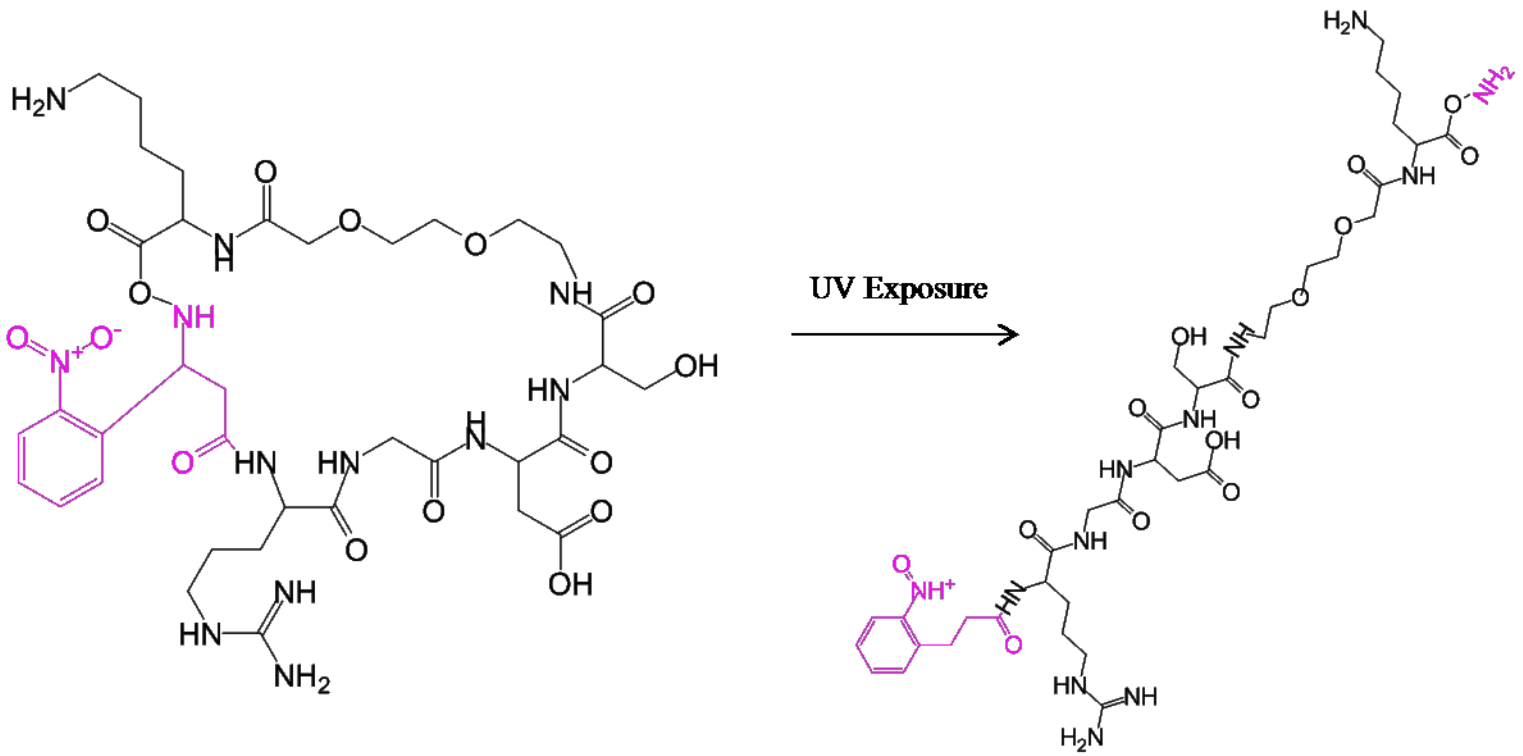

Figure 9. Photolysis reaction of cyclic caged RGDS peptide

4.2.5 Preparation of three-layered HA hydrogel

A final fermentation-derived hyaluronic acid sodium salt solution of 4 mg/ml concentration in sterile double distilled water (dd-water) was used to make HA gels. To prepare the cross-linked HA gel substrate, a solution of adipic acid dihydrazide (ADH, 15 mg) in 0.5 ml of sterile dd-water was filtered through a 0.45 μm filter and added to 10 ml of aqueous HA solution. The resulting solution was adjusted to pH 3.5 by slowly adding 1 M HCl. This was followed by the addition of 16.5 mg of filtered 1-ethyl-3-(3-dimethylaminopropyl) carbodiimide (EDC) in 1 ml of sterile dd-water with vigorous agitation. To the wells of a 12-well polystyrene tissue culture plate, 1.4 ml of the resulting reaction solution was transferred to let set. To prevent premature crosslinking, the reaction solution was cooled prior to EDC addition. Gelation was allowed to occur overnight at room temperature. The resulting gels were then washed in sterile phosphate buffered saline (PBS) solution at pH 7.4 (Invitrogen) for 24 hrs with light agitation, followed by a 24 hrs wash with dd-water. This initial HA layer was air dried for several days and two more layers of gel were deposited atop the first in the same fashion as that outlined above. Prior to use, gels were rehydrated to equilibrate in sterile PBS [66].

4.2.6 Binding peptide to HA gels

To bind peptides (both RGDS and cyclic caged RGDS) to the HA gel, a solution consisting of 25 mg/ml EDC and 15 mg/ml N-hydroxysuccinimide (NHS) in 0.1 M 2-(N-morpholino) ethane sulfonic acid (MES) buffer (pH 4.7) was prepared. Subsequently, 1 ml of this solution was added to each experimental HA gel surface that was previously transferred to and cross-linked in wells of a 12-well plate. The reaction was carried out at room temperature for 15 min to activate the carboxyl groups in

HA for peptide binding. The gels were then washed once in PBS (pH 7.4) to get rid of unreacted chemical residuals and adjust pH value. 1 ml of peptide solution (1 μmol/ml) was subsequently added to the gel surfaces and allowed to react for 2 hrs [66]. In this step, amino group on N-terminus of normal RGDS and lysine side chain amino group of cyclic caged RGDS were used to bond with activated carboxyl groups on HA hydrogels (Figure 10) [108].

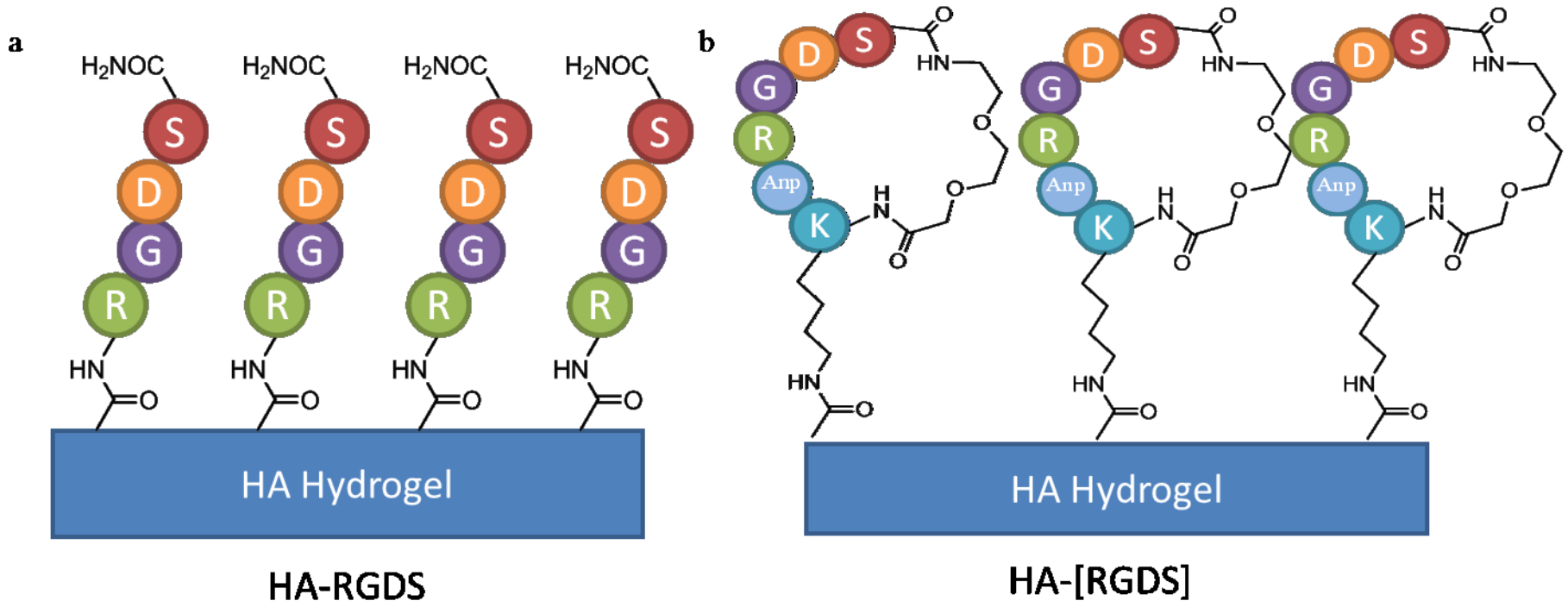

Figure 10. Schematic diagram showing cyclic caged RGDS and normal RGDS peptides bonded HA hydrogels. (a) Diagram showing the normal RGDS peptide bonded HA hydrogel through N terminus of the peptide. (b) Diagram showing the cyclic caged RGDS peptide bonded HA hydrogel through side chain amide of lysine. Amino acids were expressed by abbreviation in roundness in different colors. (R for arginine, G for glycine, D for aspartic acid, S for serine, K for lysine, Anp for Anp linker)

4.2.7 Cell study

Cell adhesion study using 3T3 fibroblasts was employed to test the efficacy of the cyclic caged RGDS peptide in modulating cell adhesion on HA surfaces before and after photo-activation. The 3T3 cells were routinely cultured in cell culture medium that was composed of Dulbecco's modified eagle medium (DMEM medium), supplemented with 10% fetal bovine serum (FBS) and 100U/ml Penicillin as well as 0.1mg/ml Streptomycin, and kept at T-25 flasks at 37℃ in a humidified environment containing 5% CO_2. For cell adhesion studies, cells were tripsinized, centrifuged, re-suspended in culture medium and counted using hemocytometer. Cells were seeded onto the experimental surfaces at a density of 1×10^4 cells/cm^2. Cell seeded surfaces were gently washed by cell culture medium to remove non-adhesion cells after 12hrs of culture. For culture examination purpose, photographs were taken, after each specific culture time period (12hrs, 2days, 4days), by an inverted phase contrast microscope (Olympus 1×81F, Richmond Hill, ON) and analyzed using Image-Pro Plus (Rockville, MD).

In order to determine that the cell adhesion was RGDS specific, in a separate study, cells were pre-incubated with 1 mg/ml of free RGDS peptide in solution before they were seeded on experimental surfaces including polystyrene (PS), HA-RGDS, and HA-[RGDS]-UV. The adherent cells from each surface were counted 12h after seeding, as previously reported [66]. Before counting the adherent cells, non-adherent cells were removed by medium renewal. Then 0.2 ml of Trypsin-EDTA solution was added to each experimental surface in 12 well plate. When the cells were observed to be detached under microscope, 0.2 ml of medium was added to each experimental surface to neutralize trypsin. Then the

cell population of each experimental group was counted separately using haemocytometer.

4.2.8 Cell morphology study

To study the cell morphology parameters, Image-Pro Plus software was used to manually trace and quantify the cell outlines in cell photographs after 48 hrs of culture. For each surface, there were at least 60 cells randomly selected from more than five different 10× magnification frames. Cell area, perimeter, aspect ratio, and roundness were automatically calculated by Image-Pro Plus as reported elsewhere [111].

4.2.9 3D Model Structure Study

Energy minimized 3D model structures of cyclic caged RGDS and uncaged RGDS peptides were computed using Hyperchem program (Gainesville, FL).

Chapter 5 Results

5.1 Mass Spectrometric Analysis

Mass spectrometric (MS) analysis was carried out to confirm the synthesis of cyclic caged peptide cyclic-(NH-Anp-Arg-Gly-Asp-Ser Adoa-Lys-CO). It was employed to monitor the products' molecular weight of crucial steps including linear peptide and cyclic caged peptide product (Steps I and III in Figure 8).

The calculated molar mass of side chain protected linear peptide, H_2N-Anp-Arg(Pbf)-Gly-Asp(OtBu)-Ser(OtBu)-Adoa-Lys(Boc)-COOH, was 1365 while ESI-MS result showed a molar mass of 1363.89m/z in Figure 12A. RP-HPLC was used to confirm that the peptide product from SPPS was in high purity (Figure 11).

Sodium and potassium attachment MS peaks were observed at 1385.87m/z and 1402.87m/z respectively while the isotope peaks for each MS were observed clearly. These salt attachment and the isotope peaks could give support to the main 1363.89m/z peak.

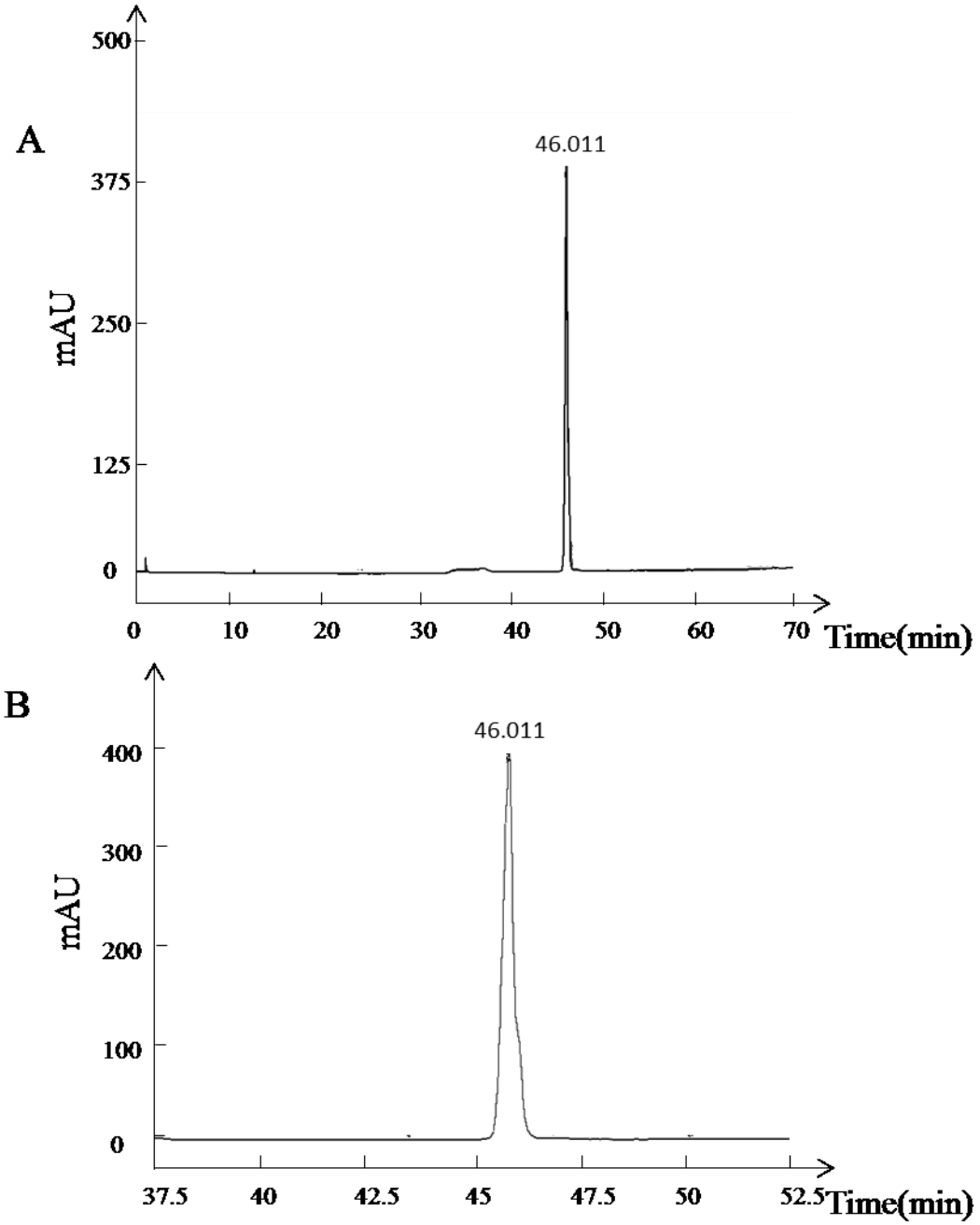

Figure 11. HPLC graph of side-chain protected linear RGDS peptide. Single HPLC peak was observed, which was a confirmation for the purity of side-chain protected linear RGDS peptide. (B) is the expansion of (A) to show shoulder peak was not observed.

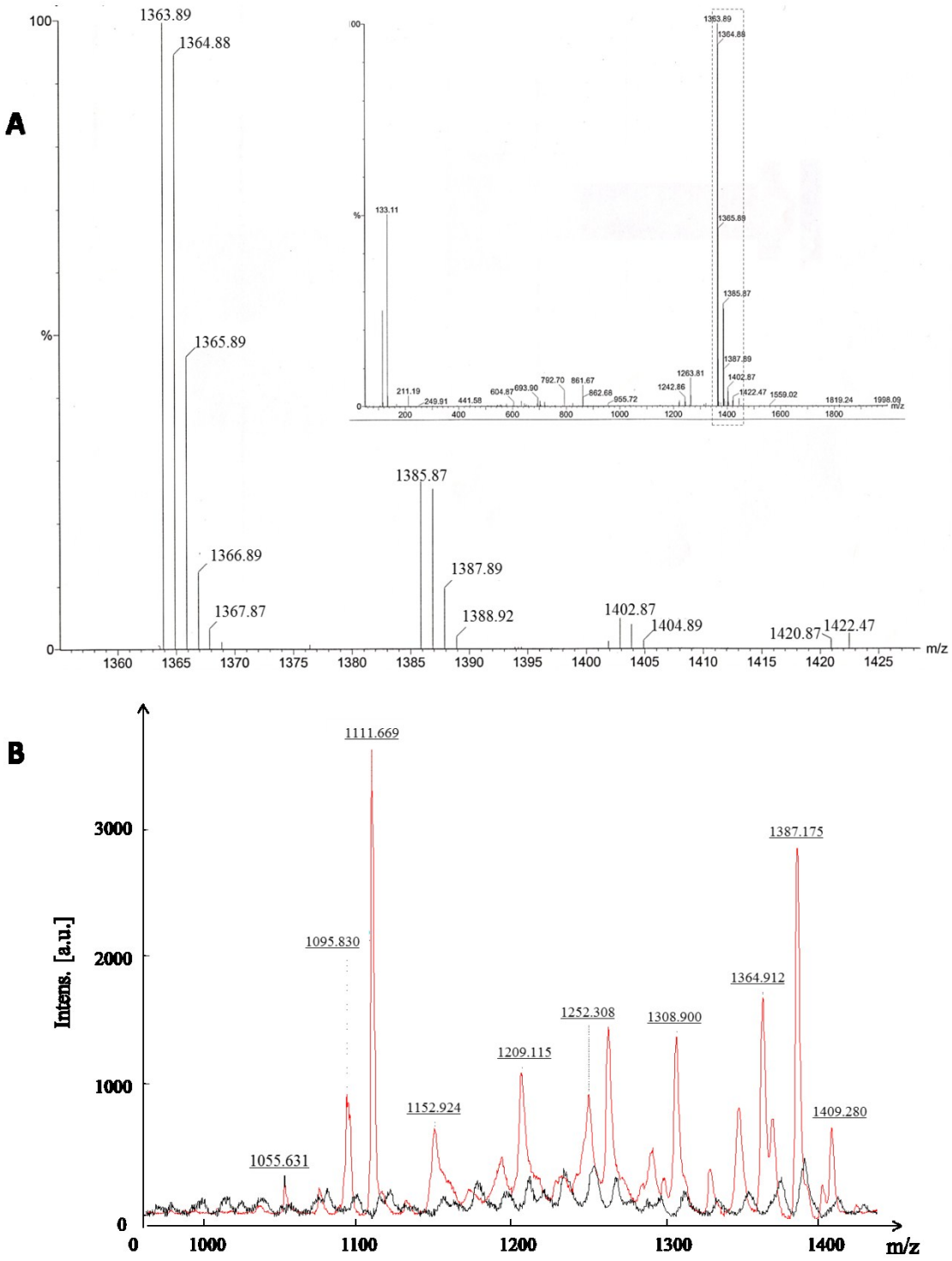

Figure 12. Mass spectrometry of linear side-chain protected peptide which theoretical molecular weight is 1387. (A) ESI-TOF MS graph showing full screen and expended mass spectrum. The expended part is pointed out by dot box. (B) MALDI-TOF MS graph showing the mass spectrum of peptide and CHCA matrix overlapped with each other

As it is shown in Figure 12B, besides original peptide peak at 1364.912 m/z, sodium attachment peak at 1387 m/z, and potassium attachment peak at 1409 m/z, many other MS peaks were also observed corresponding to peptide fragmentation. For example, 1308.9 m/z for t-butyl group (tBu) loss, 1252.308 m/z for another tBu group loss, 1111.669 m/z for 2,2,4,6,7-pentametyldihydrobenzofuran-5-sulfonyl group (Pbf) loss, and 1152.924 m/z for two tBu groups as well as a t-butyloxycarbonyl group (Boc) loss. Remarkably, these fragmentations were mostly located on side-chain protecting groups. These fragmentations during mass spectrometry not only confirmed the molecular weight of peptide compound but also confirmed its structure, for example two tBu groups confirmed the presence of glycine and aspartic; Pbf group proved the presence of arginine; and Boc group proved the presence lysine.

The ESI-MS and MALDI-MS of final product, *cyclic-(NH-Anp-Arg-Gly-Asp-Ser-Adoa-Lys-CO)*, are shown in Figure 13.

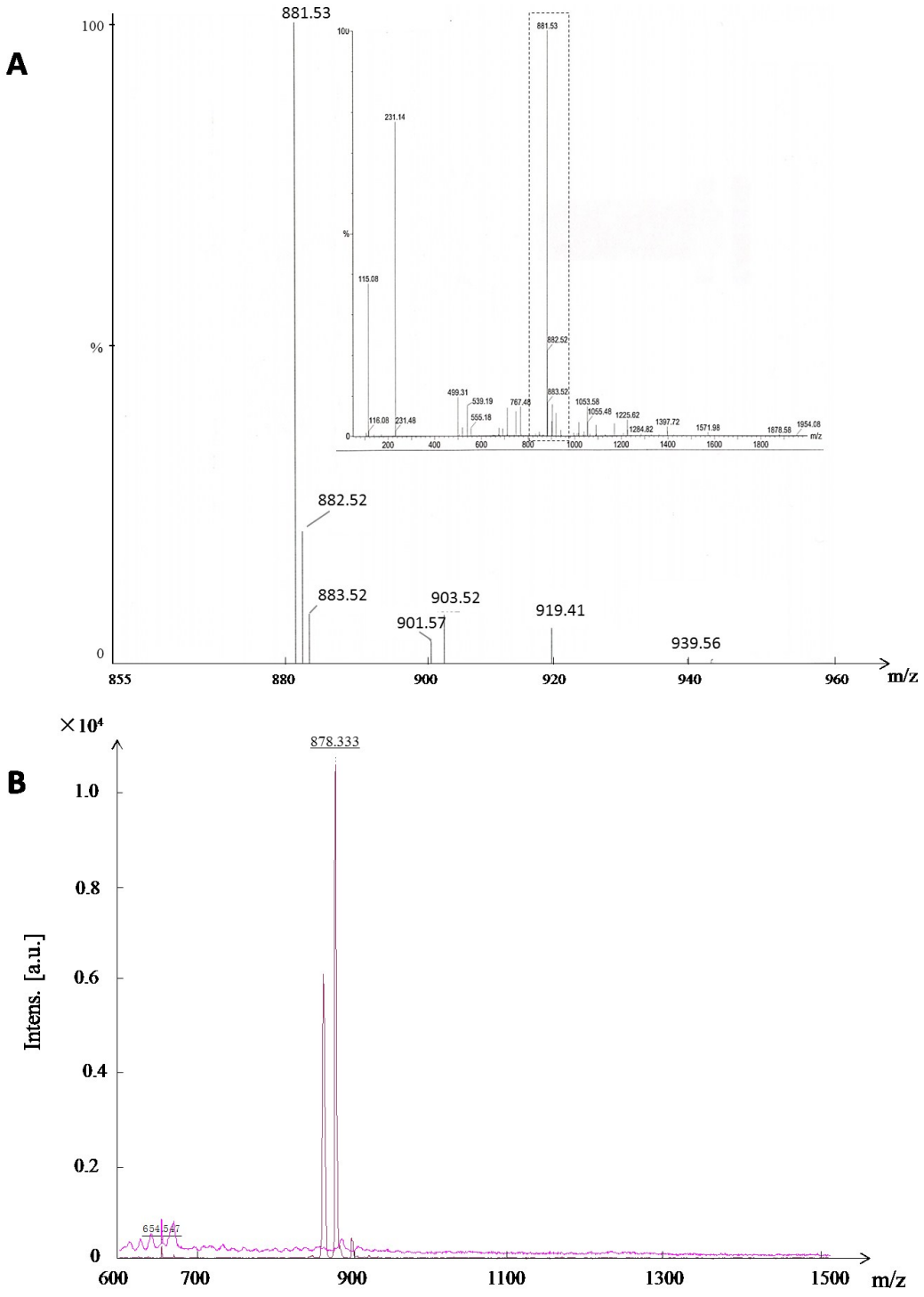

Figure 13 MS of cyclic caged RGDS peptide product which theoretical molecular weight is 881. (A) ESI-TOF MS graph showing full screen and expended mass spectrum. The expended part is pointed out by dot box. (B) MALDI-TOF MS graph showing the mass spectrum of peptide and CHCA matrix overlapped with each other

A clean ESI-MS peak was observed at 881.53 m/z for cyclic caged peptide product, which has a theoretical value of 881 (Figure 13A). This confirmed the generation of the right product during synthesis. Sodium attachment peak was observed at 903.52 m/z while potassium attachment peak was observed at 919.4 along with clear isotope peaks (881.53 m/z, 882.52 m/z, and 883.52 m/z). MALDI-MS showed exact caged peptide peak on 878.333 m/z with a 16 mass units loss peak on 863.526 m/z (for the equipment software issue, not labeled on the graph) , which was most likely a $-NH_2$ lose (Figure 13B). It was also observed that few of fragmentation occurred on the cyclic caged peptide product during MALDI-MS compared with the linear peptide sample.

Therefore, based on the mass spectrometry graphs, it could be concluded that the preparation of cyclic caged RGDS peptide was accurate.

5.2 RP-HPLC Purification

RP-HPLC purification with C-18 column was carried out to guarantee the accuracy of peptide analysis data and the reliability of cell-related studies. A single sharp peak was observed at retention time 28 minutes with C18 Phenomenex analytical column (Figure 14). This confirmed that cyclic caged peptide product was purified to HPLC grade.

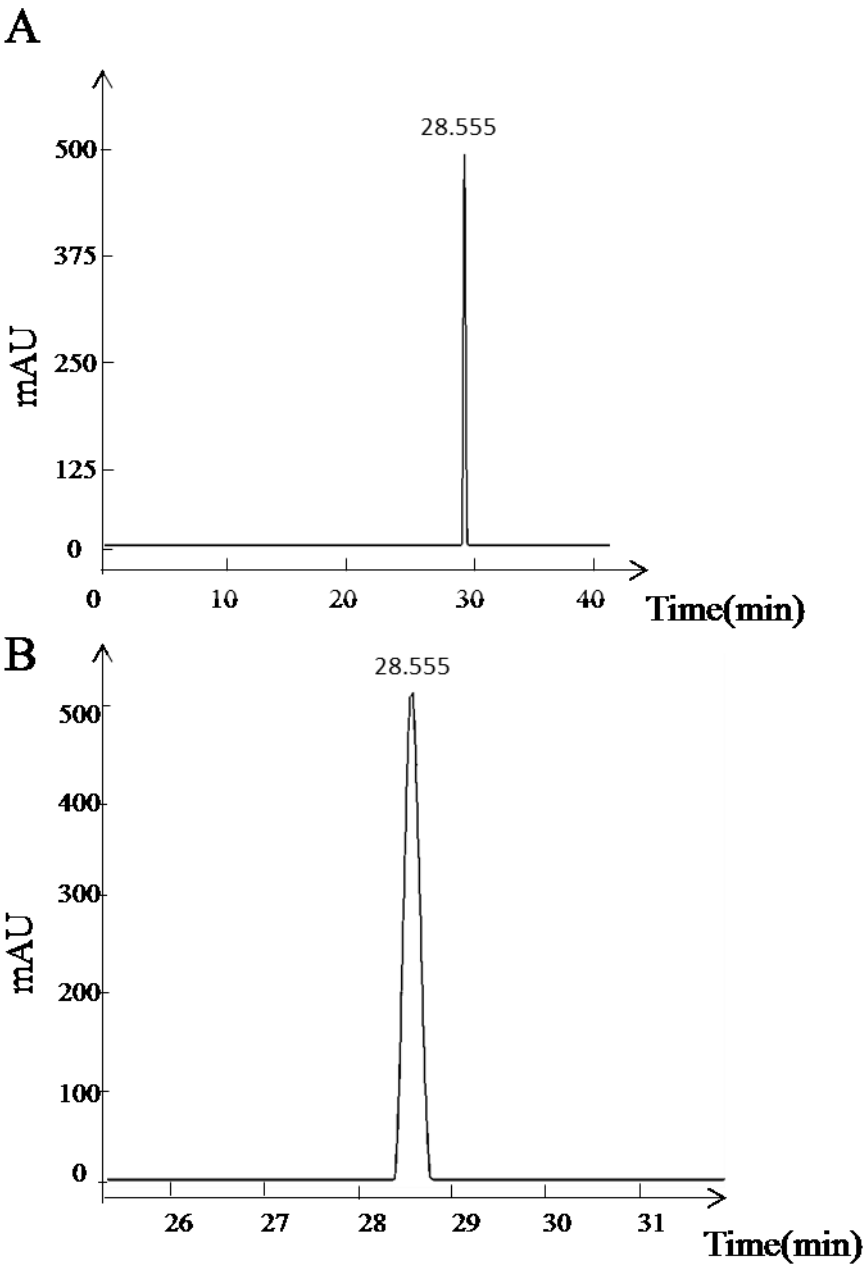

Figure 14 HPLC graph of purified cyclic caged RGDS peptide. Single HPLC peak was observed, which was a confirmation for the purity of side-chain protected linear RGDS peptide. (B) is the expansion of (A) to show shoulder peak was not observed.

5.3 Peptide Analysis

5.3.1 Circular Dichroism Spectroscopy study (CD Study)

CD study was carried out to assess the stability of peptide structure under different pH conditions. CD analysis revealed that secondary structure of cyclic caged RGDS peptide generally remained stable under different pH levels ranging from 3.5 to 8.7 (Figure 15). Furthermore, all the peptide solutions (different pH conditions) were combined and lyophilized when the CD study was accomplished. After re-dissolved with dd-water, RP-HPLC was used to remove salt and recover peptide product. Therefore, it is reasonable to assume that the cyclic caged peptide was generally stable under the pH level fluctuation in cell culture condition *in vitro*.

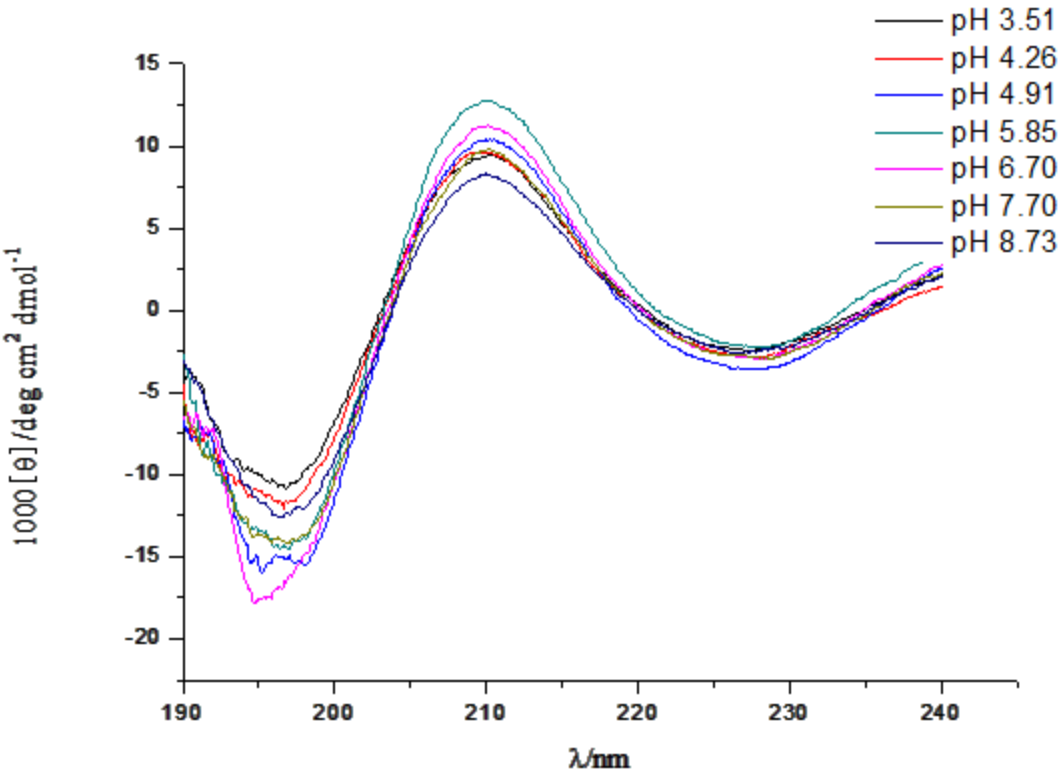

Figure 15 CD spectroscopy of cyclic caged peptide solution. Solution pH value ranges from 3.51-8.73, adjusted by 1M HCl and 1M NaOH. Spectroscopy wavelength was between 190 nm and 240 nm.

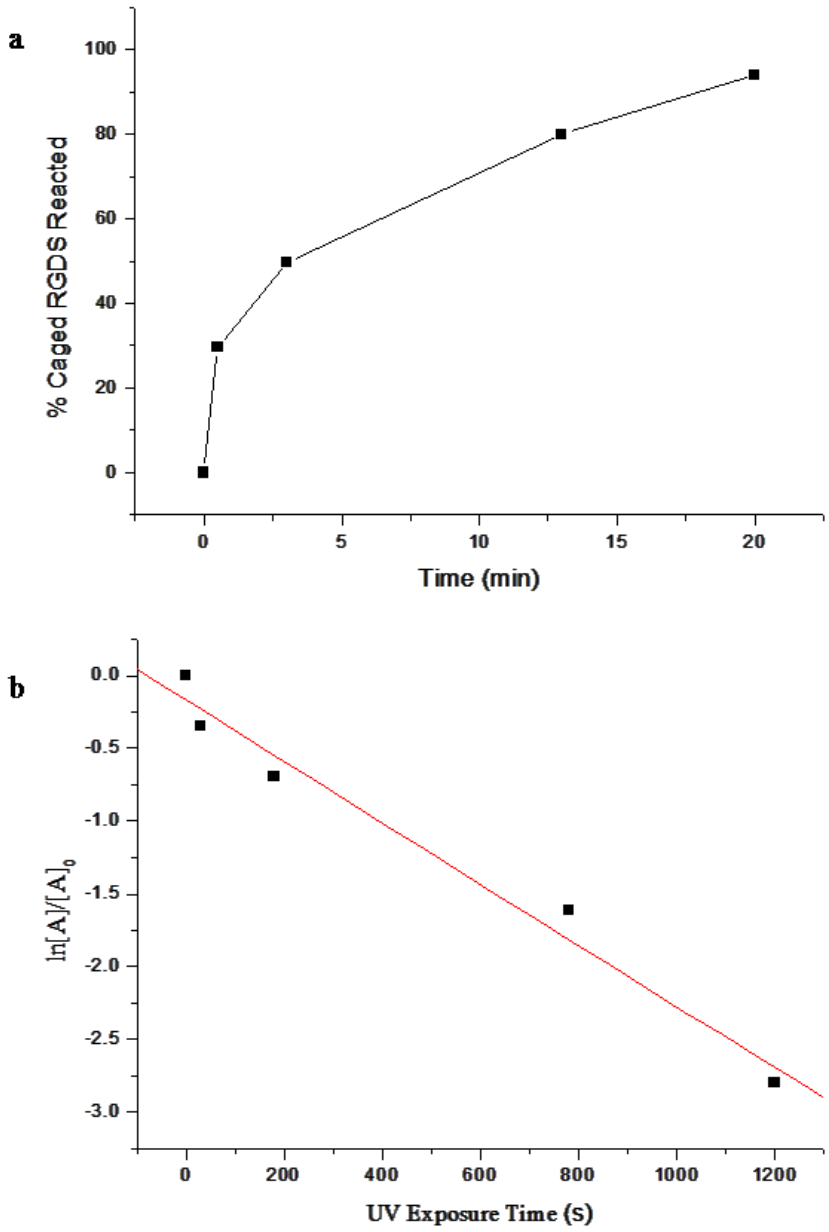

Figure 16. (a) The percentage of caged RGDS reacted with UV irradiation time. (b) Plot of $\ln[C]/[C]_o$ versus irradiation time, t. R^2=0.95. ([C]: concentration of cyclic caged RGDS peptide $[C]_o$: initial concentration)

5.3.2 Kinetic Study

Figure 16a plotted the percentage of cyclic caged RGDS reacted as a function of irradiation time, as determined from measuring the area under the cyclic caged RGDS peak in the RP-HPLC chromatograms. It was seen that after 13 min of irradiation, 80% of the cyclic caged RGDS was reacted, and over 90% of the cyclic caged peptide disappeared after 20 min. This is encouraging since it indicates that the majority of the cyclic caged RGDS reacted upon UV irradiation in 20 min. A plot of $\ln[C]/[C]_o$ versus time showed a linear relationship, which indicated that first order reaction kinetics could be used to describe the 2-nitrobenzyl photolysis as seen previously [66]. Furthermore, from Figure 16b the apparent first order uncaging reaction rate constant was calculated to be 2.11×10^{-3} s^{-1}, similar to values reported by Goubko *et.al.*, for another 2-nitrobenzyl ester compounds, which was 1.6×10^{-3} s^{-1}. Differences in the values may be attributed to differences in the solvent systems and light intensity used in the experiments [66].

5.4 Cell Study

5.4.1 Cell Attachment Study

Cell attachment was not observed on HA surface demonstrating fibroblast was not able to attach on HA hydrogel surfaces even after 4 days of cell culture (Figure 17a). Therefore, HA hydrogel surfaces could be used as black background for cell study, which was a crucial control to confirm the bioactivity of caged and uncaged RGDS peptides. In contrast, fibroblasts attached to HA-RGDS and surfaces and spread after 12 hrs' culture as well as growth after 2 and 4 days' culture, which suggested that fibroblasts

were able to recognize the RGDS peptide sequence on these HA hydrogel surfaces and specifically attached and grew on it. Fibroblasts did not attach to HA-[RGDS] surfaces and attached to HA-[RGDS]-UV, demonstrating the cyclic caging strategy sheltered the bio-activity of RGDS peptide. Schematic diagram showing UV uncaging reaction of cyclic caged RGDS peptide on HA hydrogel is given in Figure 17c.

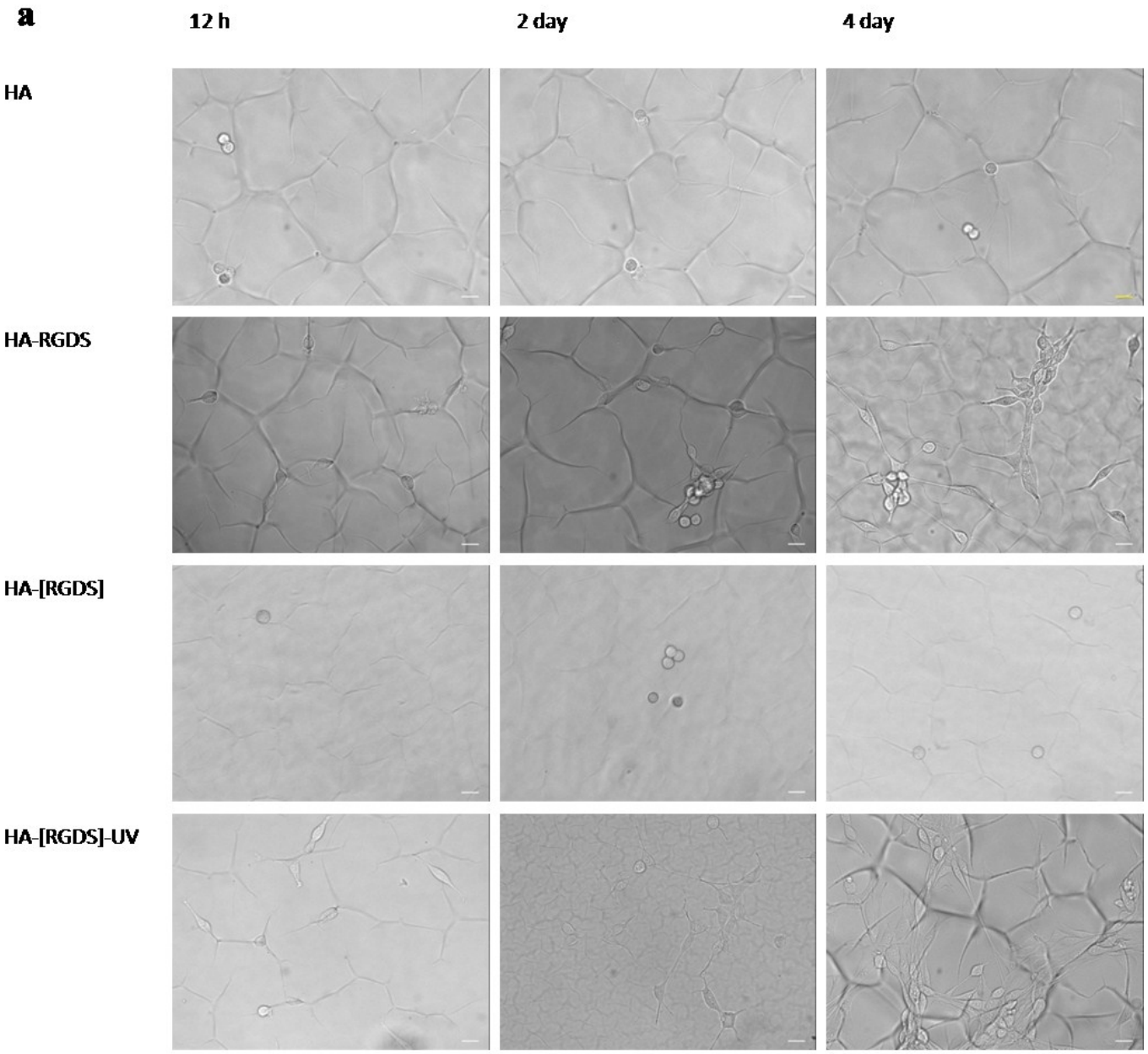

Figure 17. (a) Photograph result of cell attachment study. Each horizontal line corresponding to an experimental group and each vertical column represents a culture time. Photos were taken at 12 hours, 2 days and four days after cells were seeded. HA hydrogel surface was selected as negative control and normal RGDS coated HA surface was selected as positive control. Bar is 20 μm.

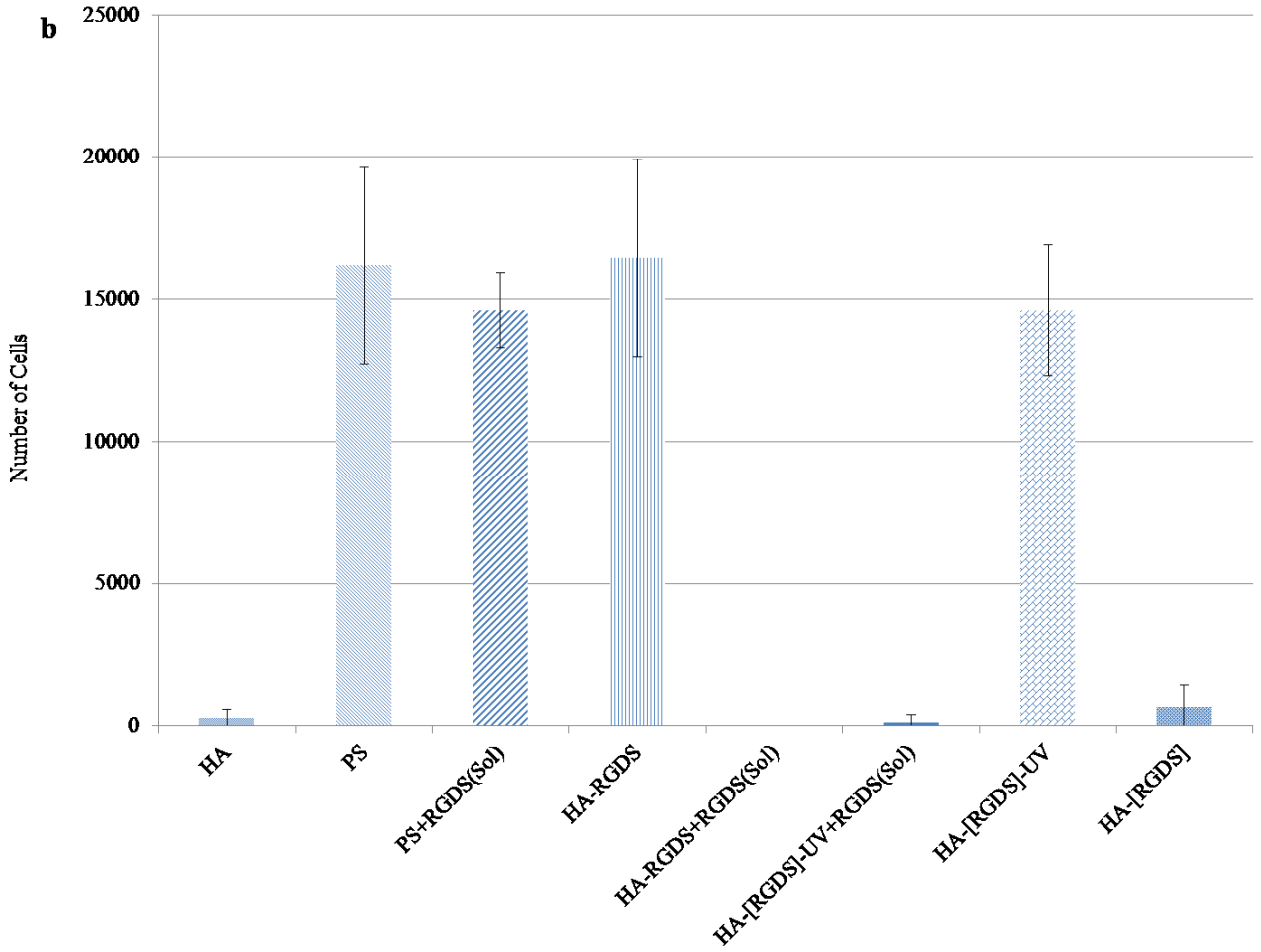

Figure 17. (b) Bar diagram showing cell counting study. Cell population was counted at 12 hours after cells were seeded. RGDS(Sol) represents the control group with free RGDS peptide dissolved in tissue culture medium. It is to confirm the cell attachment was RGDS-dependent. Polystyrene tissue culture plate was selected as positive control and HA hydrogel surface was selected as negative control. Error bars representing one standard deviation from the mean.

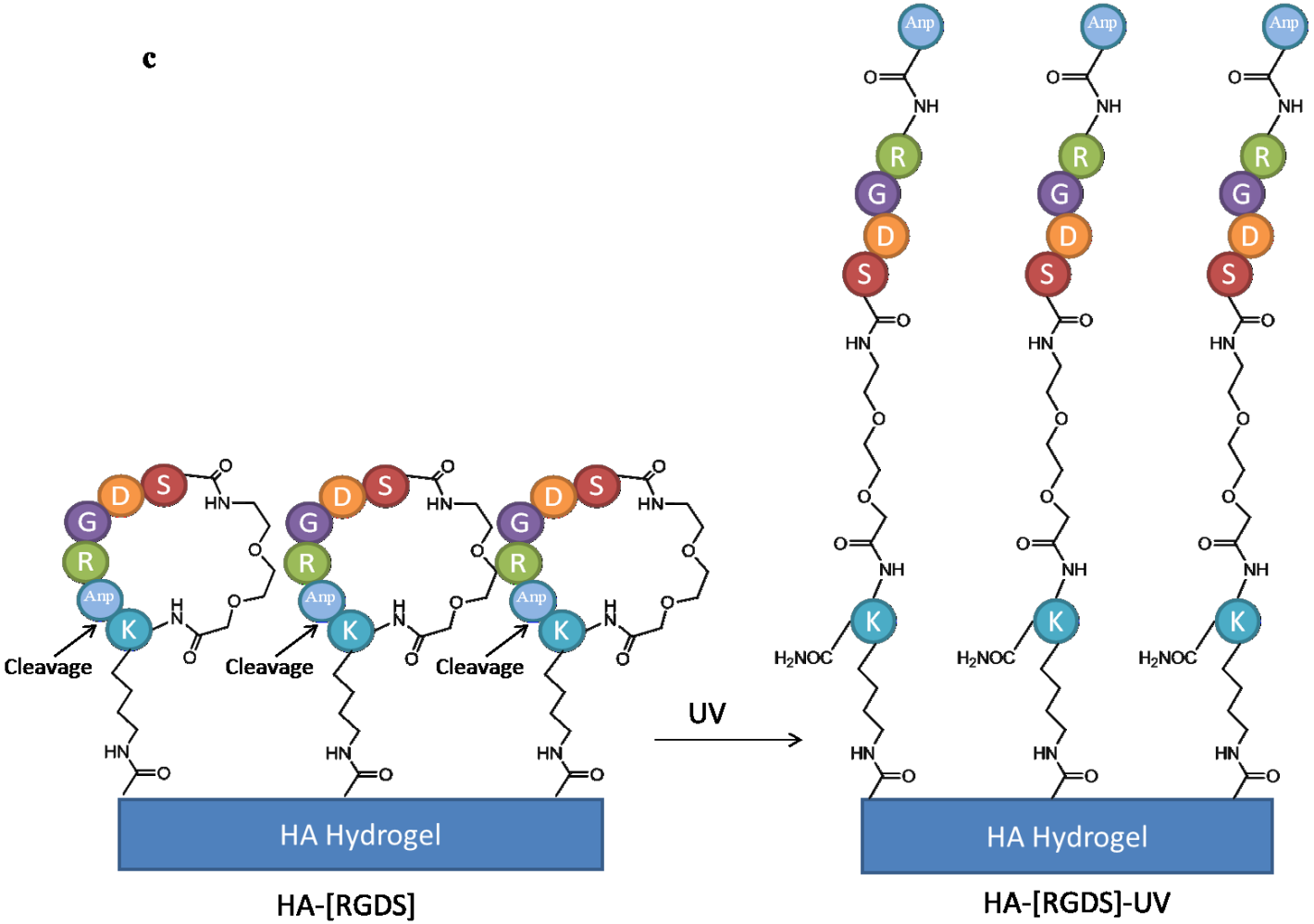

Figure 17 (c) Schematic diagram showing UV uncaging reaction of cyclic caged RGDS peptide on HA hydrogel. Amino acids are expressed by abbreviation in roundness in different colors. The cleavage position of cyclic caged RGDS peptide upon UV exposure is indicated by arrow.

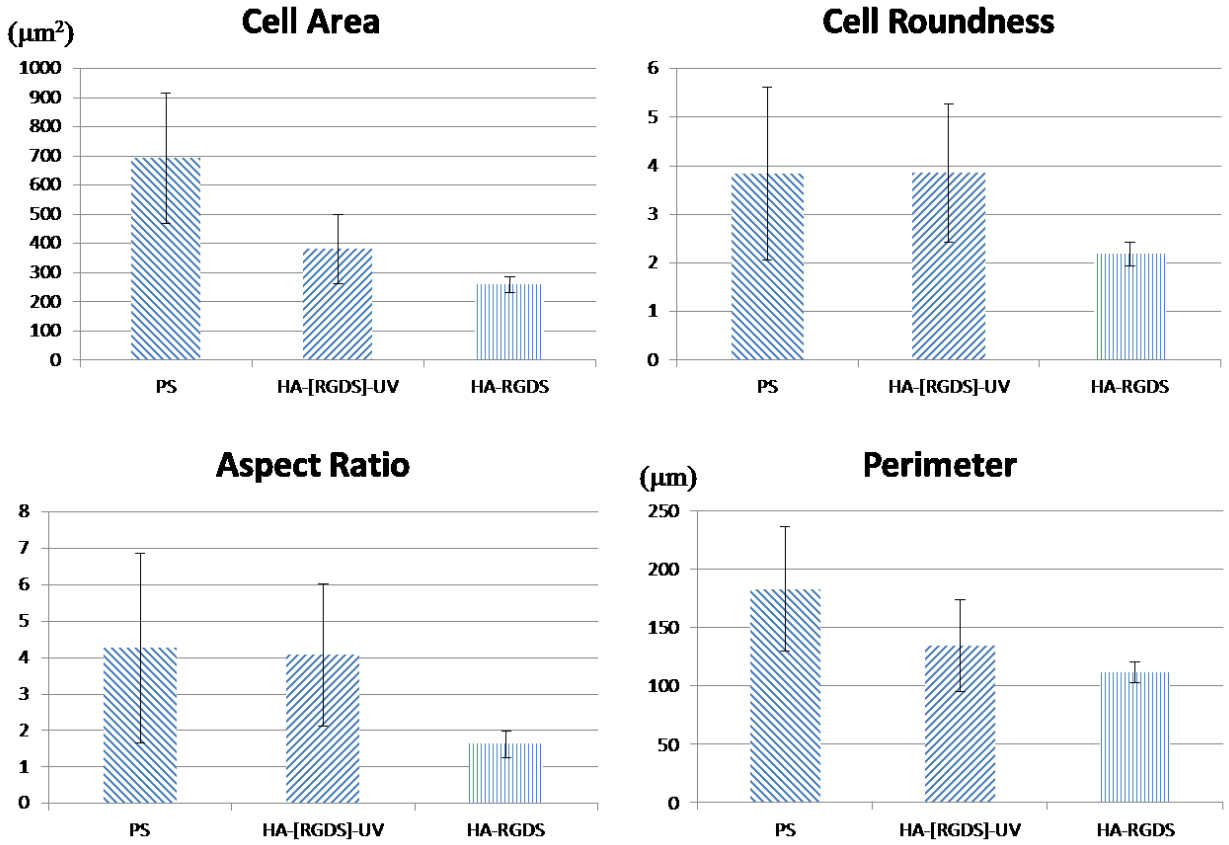

Figure 18 Bar diagram showing different cell morphology study for uncaged RGDS peptide and normal RGDS peptide bonded HA surfaces. Four parameters were selected (cell area, cell roundness, aspect ratio and perimeter). Morphology data was collected by Image-Pro software at 48 hours after cells were seeded. Polystyrene tissue culture plate was selected as positive control. Error bars representing one standard deviation from the mean.

5.4.2 Cell Counting

To quantify the cell attachment, cell counting experiment was implemented to each specific experimental surface. Moreover, to determine the statistically significant differences among specific experimental groups, one-way ANOVA (significant level 0.05) study was applied. Cell counting study showed similar numbers ($p>0.05$, not significant different) on HA-RGDS surface and on PS tissue culture plate which indicated an outstanding biocompatibility for the peptide modified HA material (Figure 17b). The amount of cells attached to HA-[RGDS]-UV surface was slightly less than it was for PS surface, suggesting that the peptide uncaging reaction under UV exposure was not totally completed and very little amount of RGDS peptide may still remain caged. The difference between them was not significant ($p>0.05$), which suggesting the yield of uncaging reaction was acceptable. Comparing with PS tissue culture plate, a significantly smaller amount of cells were counted on HA hydrogel surface and HA-[RGDS] surface ($p<0.05$) suggesting the cyclic caging strategy indeed inhibited cell attachment to the RGDS peptide. In order to further confirm that the cell binding was modulated by RGDS peptide sequence, cell counting studies were implemented to the surfaces of HA-RGDS, HA-[RGDS]-UV with the presence of free RGDS peptide in the tissue culture medium. Results obtained from the study (Figure 17 b) suggested that the peptide modified surface attachment of fibroblasts could be completely inhibited by the presence of free RGDS peptide in the concentration of 1mg/ml. Comparing with the PS tissue culture plate, the cell population difference was significant ($p<0.05$). This demonstrated that the cell attachment behavior was integrin dependent (free RGDS peptide blocked the specific cell receptors and made them unable to facilitate the cell attachment behavior). In addition, to confirm the normal behavior of

fibroblast in the presence of free RGDS peptide, free RGDS presence cell counting study was also applied to the PS cell culture plate. Comparing to original PS group, the difference of cell population was not significant ($p>0.05$, Figure 17b).

5.4.3 Cell morphology study

Cell morphology study was applied at 48 hrs after the cells were seeded to figure out how cells behaved with each specific experimental surface[111]. Four morphology parameters were studied, which were cell perimeter, mean cell area, cell roundness, and aspect ratio (Figure 18).

Moreover, to determine the statistically significant differences of each specific experimental group, one-way ANOVA (significant level 0.05) study was applied. The result revealed that, the cells were attached to HA hydrogel surface when modified with RGDS peptide and the differences between PS based cell adhesion and RGDS based cell adhesion were significant ($p<0.05$). This indicated that, on RGDS modified HA hydrogel surface, fibroblast didn't spread to the level as good as it was on polystyrene surface. However, the cell morphology data suggested that differences in cell roundness and aspect ratio between polystyrene and uncaged-RGDS peptide were not significant ($p>0.05$), but there were still significant differences in the parameters of cell perimeter and mean cell area ($p<0.05$). In addition, the differences on cell aspect ratio and cell roundness were also significant ($p<0.05$), which means on uncaged RGDS coated HA surface cells could spread better than they were on normal RGDS coated HA surfaces.

5.5 3D Molecule Modeling

A general view showing the 3D model structure of the cyclic caged RGDS peptide in its lowest

possible energy state is depicted in Figure 19a. Though completely theoretical and generated under solvent free condition, it provides some important information about the salient features of the structure [112]. Thus, it was noted that there were two potential hydrogen bonds formed that likely participated in the stabilization of the obtained structure. Both hydrogen bonds were displayed in figures as dotted bonds in order to differentiate from normal covalent bonds. One of the hydrogen bonds labelled as H_1 in the figure was formed between the backbone amide nitrogen of aspartic acid and the hydrogen of backbone amide bond of serine residue. The second hydrogen bond labelled as H_2 was formed between the nitrogen on adoa residue and the hydrogen atom of the amide bond of anp linker. Interestingly in both cases the hydrogen atom implicated in the bond is situated between two electro donating nitrogen atoms. Oxygen atoms didn't provide any significant contribution to the formation of these hydrogen bonds. The modeling figures showing the formation of hydrogen bonds H_1 and H_2 were shown more distinctly in the enlarged figures (Figure 19c and Figure 19d respectively). These two hydrogen bonds not only stabilized the rigid cyclic structure but also provided a narrow hole of the peptide ring. In Figure 19b, the backbone of RGDS sequence with the names of the amino acids involved were labeled for easy visualization. Our model figure also demonstrated that the back bone structure of RGDS was more widely bent and all the side chain functional groups were well projected out of the peptide ring in different directions in a divergent manner. Remarkably, the side chain of lysine, located between arginine and glycine residues, most probably disrupted the RGDS structure and the receptor recognition in cell attachment study. The overview of uncaged RGDS 3D model structure was shown in Figure 19e. It was observed from the figure that the cyclic caging ring was opened and the two hydrogen bonds as indicated above for the cyclic peptide were destroyed upon UV uncaging reaction. The backbone pattern of the RGDS sequence (Figure 19f) became more flat and

sheet like compared with the corresponding cyclic one. Besides, the side chain of lysine and the aromatic ring of anp linker were located inside the semi-cyclic ring generated by the peptide backbone, which could no longer alter the structure of RGDS peptide in a significant manner. In addition, the side chains of RGDS sequence were projected outside the semi-cyclic ring and close to each other, which probably made the peptide much easier to be recognized by the receptor [112].

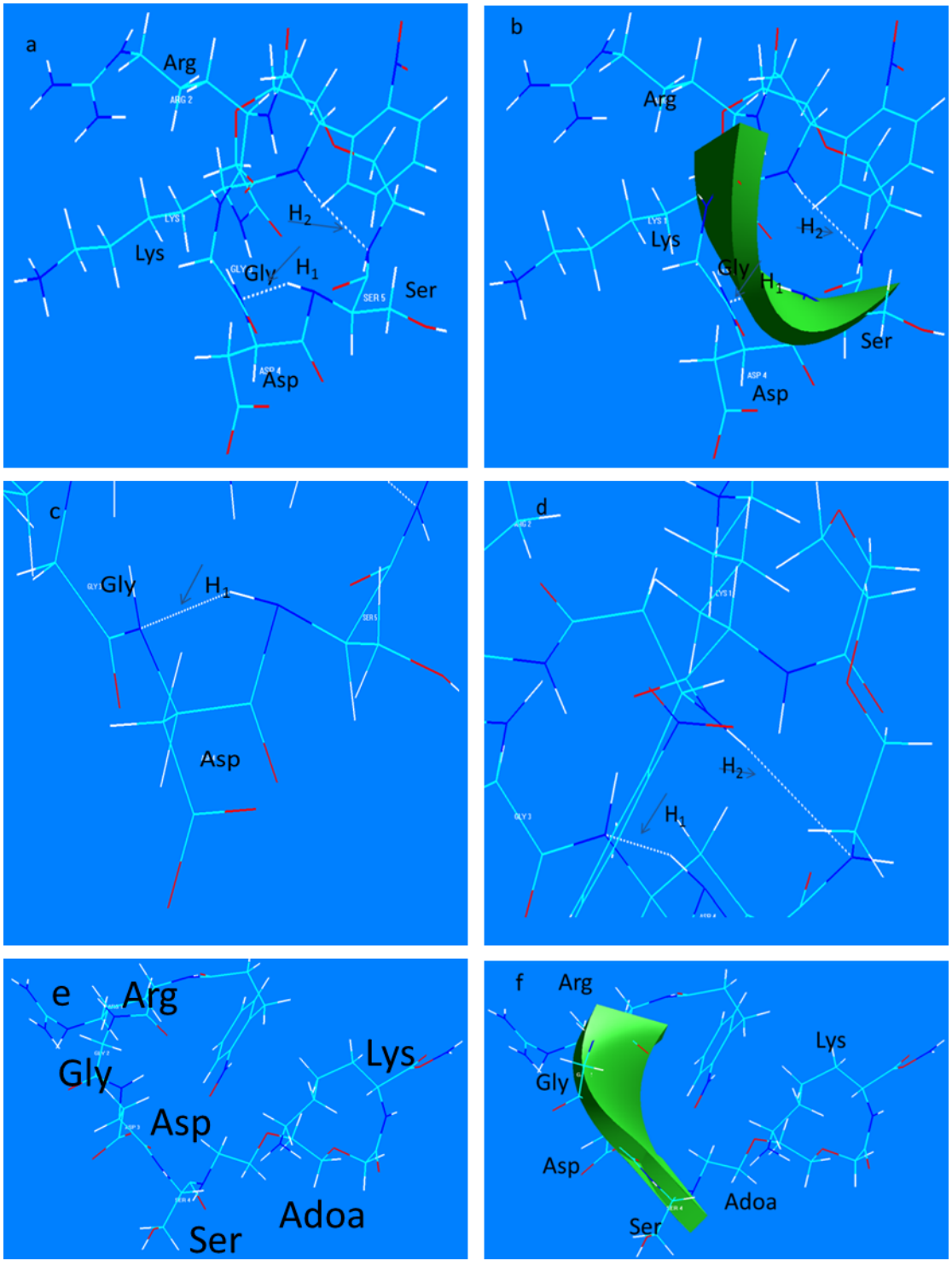

Figure 19. 3D model structures of cyclic caged RGDS peptide and uncaged RGDS peptide. H_1 and H_2 represent the two hydrogen bonds. The backbone pattern of RGDS sequence is shown by green sheet. a) represents the general view of cyclic caged RGDS peptide. b) shows the backbone pattern of a). c) and d) are zoom in of a) representing the two hydrogen bonds H_1 and H_2. e) represents the general view of uncaged RGDS peptide. f) shows the backbone pattern of e).

Chapter 6 Discussion

6.1 Peptide Synthesis

Several strategies have been used to cage RGD peptides and make it photo-active. Goubko reported that 2-nitrobenzylamine hydrochloride could be used to photo-labile cage the biological activity of RGDS when bonded to carboxyl side chain of aspartic acid [87]. This was confirmed by cell attachment study on peptide modified HA hydrogel surfaces. Besides, 3-(4,5-dimethoxy-2-nitrophenyl)-2-butyl was used to photo-labile control the bio-activity of cyclo(RGD) peptide when bonded to the carboxyl side chain of aspartic acid [108, 113]. It was confirmed by cell attachment study on peptide modified silica surfaces. Although each of them had its specific advantages, all of them had the same issue, their synthesis steps were complex. This was generally caused by their core idea to cage an amino acid and then use the caged amino acid to synthesize the caged peptide. This core idea could inevitably result in the following disadvantages:

- ✓ An extra purification step is needed when caged amino acid is synthesized.
- ✓ The coupling reaction of caged amino acid and normal amino acid would be extraordinarily hard for the effect of caging group stereo hindrance. This can directly lead to low yield and complex reaction operation steps.

To synthesize the caged peptide by the above strategies, these disadvantages could directly lead to extensive time and reagent consumption, low yield and low reproducibility. Therefore, the strategy designed and applied in this thesis was based on a completely different core idea, which has never been

reported in the field of caging RGDS peptide sequences. With the assistance of automatic SPPS machine, the raw peptide product was prepared easily in large scale with undoubtedly high yield, purity and less time consumption. In addition, based on the fact that it is side chain protected peptide and the N-terminus of Anp linker is still free [63], this peptide is usually stable in solid state which is achieved by lyophilisation. Starting from this raw peptide product, there were two manual operation steps followed in the study to make the caged peptide ready to use.

6.2 RP-HPLC purification

RP-HPLC with C18 Phenomemex semi-analytical column was applied to purify the final product after cyclic caging reaction and deprotection. The column used for purification was semi-analytical column while the one to confirm the peptide purity was analytical column. Five compound peaks were observed, with retention time of 22.232, 24.293, 25.016, 25.387, and 27.187 min as shown in Figure 20. MALDI-MS and ESI-MS were also used to detect the molecular weight of these five compounds. The compound with retention time 22.232 min was confirmed to be crude linear peptide. Unexpectedly, mass spectrum gave the same molecular weight for the last four of them, which was the molecular weight of the desired cyclic caged peptide compound. In consideration of the technique used to prepare this compound, it was very likely that all these four HPLC peaks were given by the same compound, the cyclic caged peptide.

Thus, the question of four separate HPLC peaks shown by peptide compound needs to be answered. The major reason assumed to explain the ‘four separate HPLC peaks issue’ was chiral isomer. Studying the structure of the cyclic caged peptide, it is easy to find out that there are two possibly chiral centers as shown in Figure 21, which could divide one HPLC peak into four.

a. The carbon in Anp linker connecting the N-terminus, C-terminus, and aromatic ring could be a chiral center when N-terminus was reacted. The HPLC peak split, caused by Anp linker, was also reported by other studies recently [110].

b. Another chiral center was most likely located at the center carbon of serine amino acid. Even though all the amino acids used for peptide synthesis were L-amino acids, the racemization could still occur to the L-serine with the presence of concentrated alkali during cyclic caging reaction. Detailed mechanism of the racemization is shown in Figure 22 [114].

^{1}HNMR is one of the best options to confirm the racemization assumption, however, due to purification difficulty for HPLC peaks during 24.293-25.387 minutes, a ^{1}HNMR graph good enough to be a proof for this was not obtained.

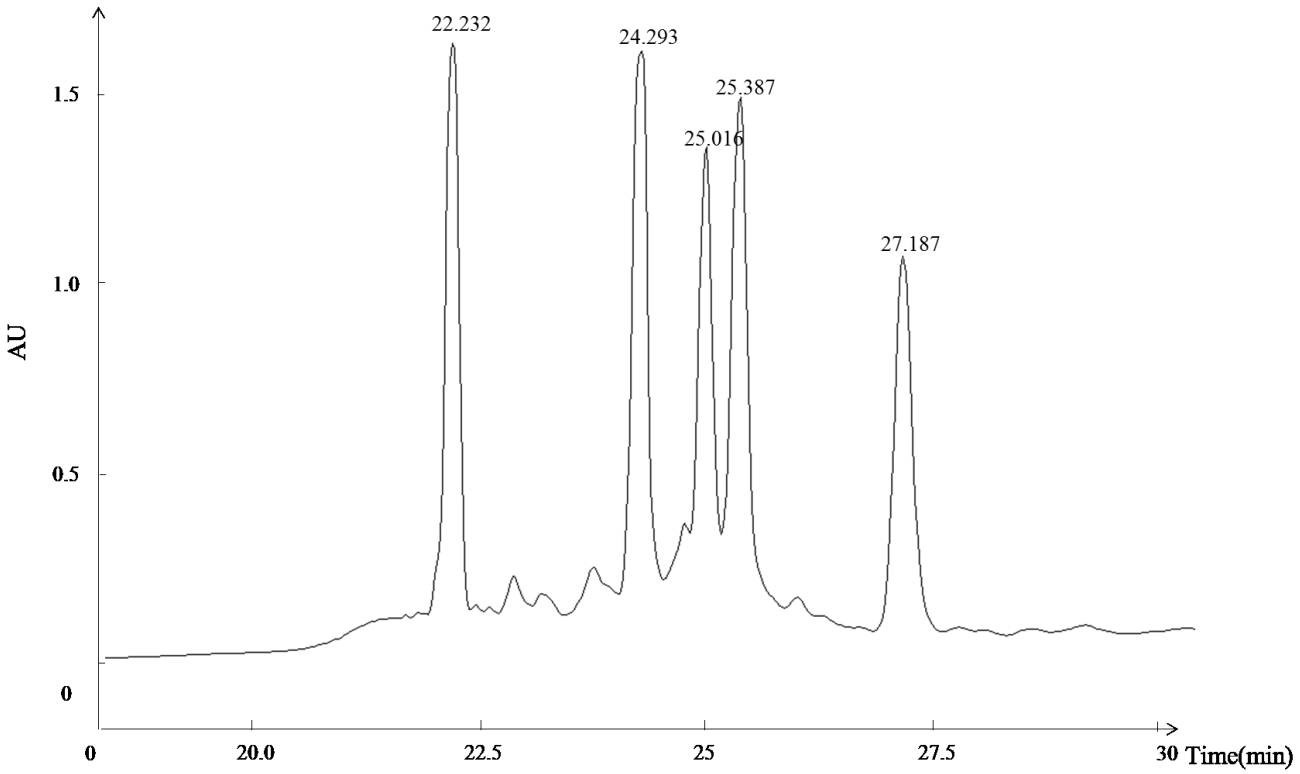

Figure 20. RP-HPLC graph showing purification for cyclic-caged peptide. Five peaks were observed on retention time 22.232, 24.293, 25.016, 25.387, and 27.187 minutes. 22.232 minute peak is linear peptide peak, and the rest four peaks are caused by two chiral centers in cyclic caged RGDS peptide.

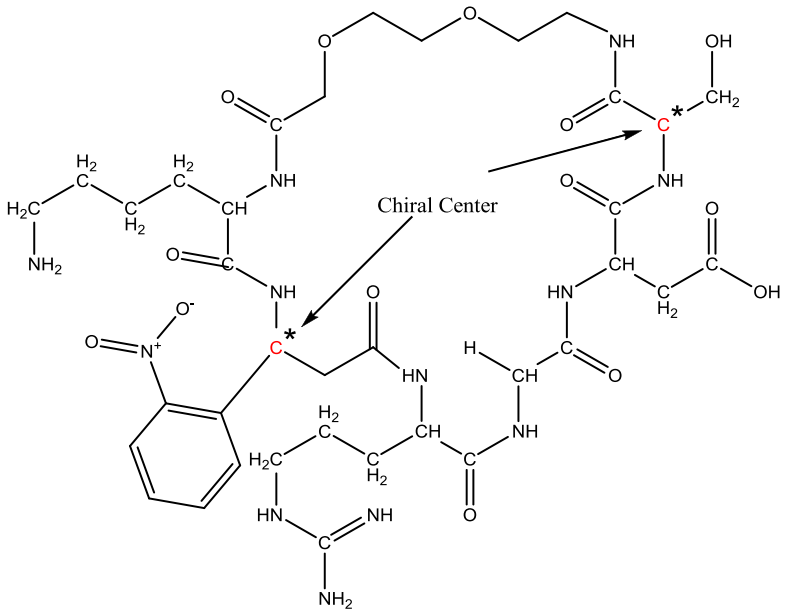

Figure 21 Chemical structure showing chiral centers of cyclic caged RGDS peptide (the carbon in Anp linker connecting the N-terminus, C-terminus, and aromatic ring as well as the center carbon of serine amino acid). The chiral centers are highlighted by arrows and stars.

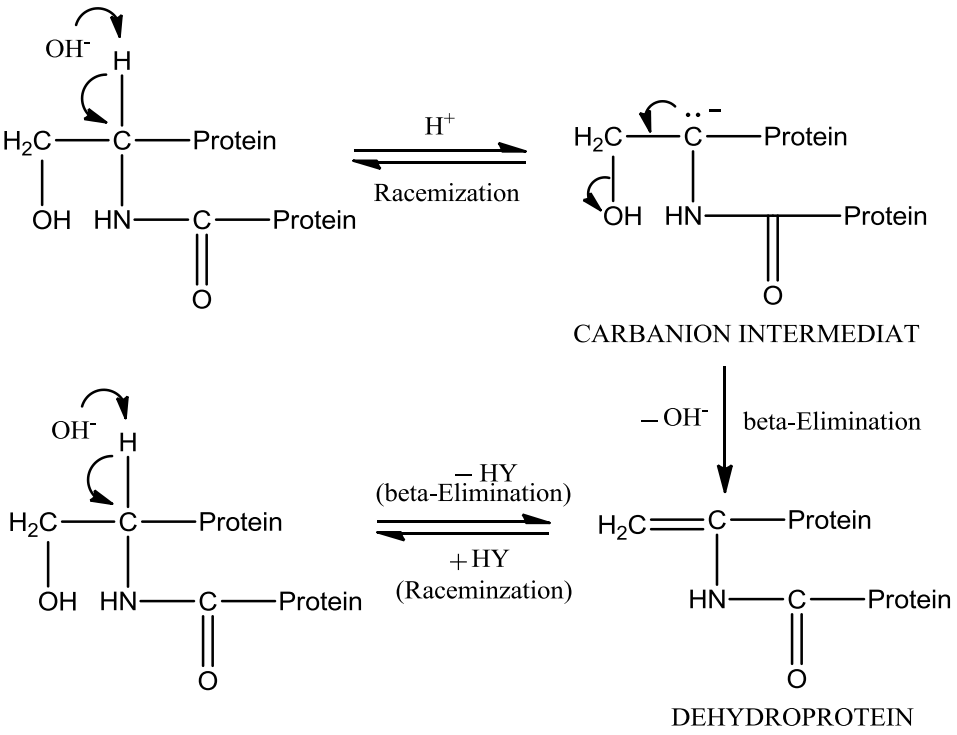

Figure 22 Schematic diagram showing racemization of Serine

6.3 Cell Morphology Study

During the cell morphology study, regarding to the aspect ratio and cell roundness, it was observed that cells were spread better on the uncaged peptide coated HA surfaces rather than normal RGDS peptide coated HA surfaces. This phenomenon was most probably caused by the different ways that RGDS peptide sequences were bonded to the solid phase HA surfaces.

When normal RGDS was bonded to HA, the N-terminus of arginine was directly employed, however, the RGDS sequence of uncaged RGDS peptide was 16 molecules away from the main solid phase when bonded with HA. It has been studied that RGDS peptides showed various cell-adhesion properties when they were in different 3D configurations [34]. Linkers were normally employed to get more suitable 3D configuration, enhance the cell attachment property of RGDS peptide, and decrease steric hindrance [108, 113].Therefore, when bonded to HA surface, the RGDS sequence of uncaged peptide was in much less steric hindrance compared to the one of normal RGDS as shown in Figure 23 and the flexibility directly lead to the better adhesion behavior [115].

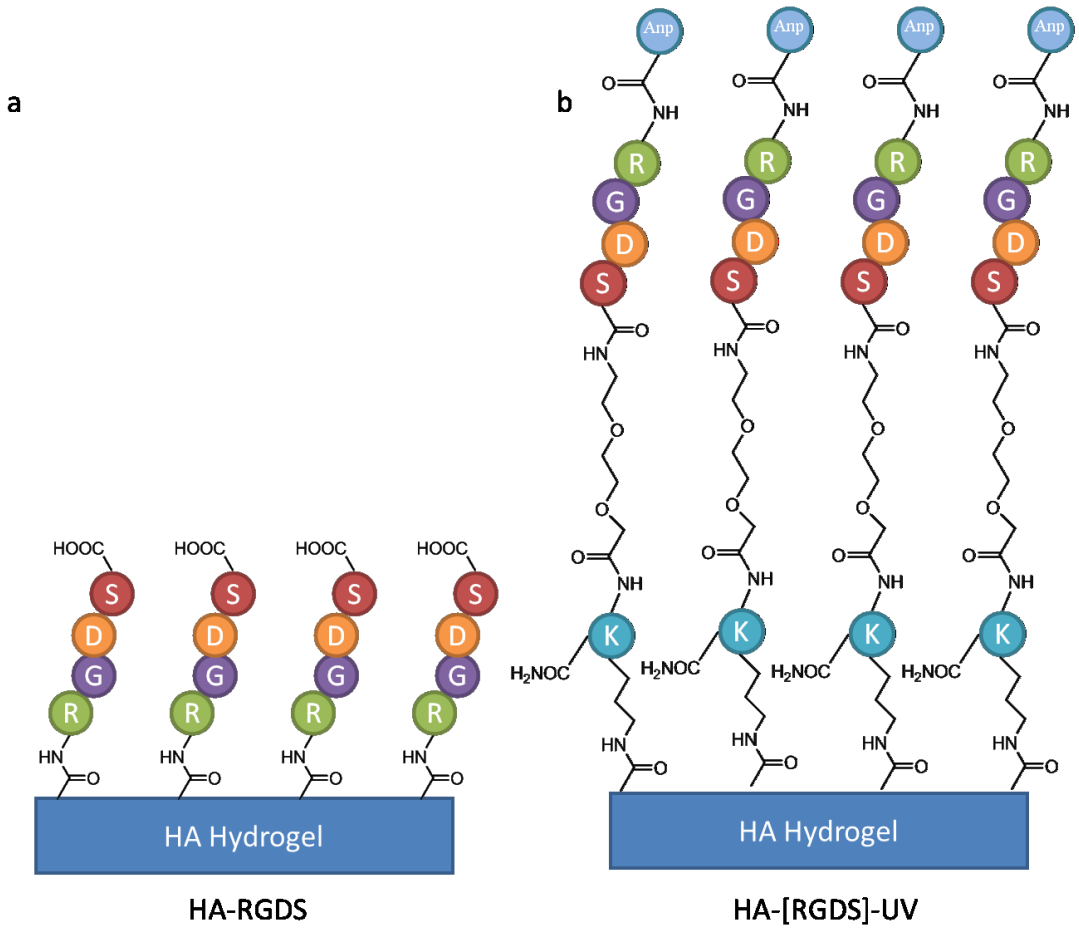

Figure 23 Schematic diagram showing normal RGDS and uncaged RGDS peptide bonded HA hydrogel. Amino acids are expressed by abbreviation in roundness in different colors. (a) Normal RGDS bonded HA hydrogel. (b) Uncaged RGDS bonded HA hydrogel.

6.4 Summary

Besides above RGDS peptide caging strategy, there were several other similar approaches had been applied. For example, Goubko *et. al.* reported caged RGDS peptide by caging 2-nitrobenzyl group on the side chain of Gly. The related cell attachment study on peptide coated HA surfaces were also reported [66, 87]. Petersen *et. al.* also reported carboxyl side-chain blocked photo-labile caged cyclo(-Arg-Gly-Asp-d-Phe-Val-) peptide and its related cell patterning study [108]. Wirkner *et. al.* made another approach which was similar to Petersen's in 2011 [113]. But none of them could avoid the trouble caused by steric hindrance during the synthesis procedures and majorly made use of automatic peptide synthesize mathine due to their caging strategy issue.

Another remarkable approach need to be mentioned is that Umezawa *et. al.* also accomplished several cyclic photo-labile peptides by Anp linker, which was similar to the strategy used in this article [50]. However, the related biological studies has not been reported.

Chapter 7 Conclusions and Future Work

We have developed a novel photo-labile caged RGDS peptide with cyclic caging strategy and confirmed the biological activity of caged and uncaged peptide on a non-adhesive hyaluronic acid hydrogel surface. To form the cyclic caging, N-terminus of arginine and C-terminus of lysine were connected by Anp linker, which was cleaved by UV exposure. We were able to confirm the 1^{st} order reaction of photolysis reaction and stability of the caged peptide in various pH values. Moreover, after bonded with the caged peptide, hydrogel surface was non-adhesive to cells, but could be switched to become cell adhesive upon exposure to UV light. Cell counting study and morphology study were also applied to demonstrate the extent of the adhesion to various modified hydrogel surfaces. Besides, it was also confirmed that the adhesion of uncaged peptide surface was due to RGDS receptor by the study of suspension free RGDS peptide in the cell culture medium.

For this research, several goals as given below are still needed to be achieved in the future:

1. The stability of cyclic caged RGDS in aqueous environment is needed to be compared with other similar caged RGDS peptides.
2. The amount of peptide bonded to the HA surface after previous protocol is needed to be studied.
3. Cell patterning study is needed to be carried out in two and three dimensional biomaterial.
4. Biological evaluation on neuron cells for caged and uncaged RGDS should be implemented.

References

1. Venes, D., B.G. Fenton, and C.W. Taber, *Taber's Cyclopedic Medical Dictionary (Thumb-Indexed Version)*. 2013: Medicus Media.
2. Brieke, C., et al., *Light-controlled tools.* Angewandte Chemie-International Edition, 2012. **51**(34): p. 8446-8476.
3. Blackwell, T.L., *Spinal cord injury desk reference: guidelines for life care planning and case management*. 2001: Demos Medical Publishing.
4. Campagnolo, D.I., et al., *Spinal Cord Medicine*. 2011: Wolters Kluwer Health.
5. Canada, S.C.I. 2013 [cited 2013 29 August]; Available from: http://www.lse.ac.uk/library/services/training/endnote/Quick%20Tip%20citing%20webpages.aspx.
6. Varma, A.K., et al., *Spinal cord injury: a review of current therapy, future treatments, and basic science frontiers.* Neurochemical Research, 2013. **38**(5): p. 895-905.
7. Jackson, K.A., et al., *Regeneration of ischemic cardiac muscle and vascular endothelium by adult stem cells.* J Clin Invest, 2001. **107**(11): p. 1395-402.
8. Horner, P.J. and F.H. Gage, *Regenerating the damaged central nervous system.* Nature, 2000. **407**(6807): p. 963-70.
9. Liu, S., et al., *Embryonic stem cells differentiate into oligodendrocytes and myelinate in culture and after spinal cord transplantation.* Proc Natl Acad Sci U S A, 2000. **97**(11): p. 6126-31.
10. Billon, N., C. Jolicoeur, and M. Raff, *Generation and characterization of oligodendrocytes from lineage-selectable embryonic stem cells in vitro.* Methods Mol Biol, 2006. **330**: p. 15-32.
11. Deshpande, D.M., et al., *Recovery from paralysis in adult rats using embryonic stem cells.* Ann Neurol, 2006. **60**(1): p. 32-44.
12. Nandoe Tewarie, R.S., et al., *Stem cell-based therapies for spinal cord injury.* J Spinal Cord Med, 2009. **32**(2): p. 105-14.
13. Nistor, G.I., et al., *Human embryonic stem cells differentiate into oligodendrocytes in high purity and myelinate after spinal cord transplantation.* Glia, 2005. **49**(3): p. 385-96.
14. Sharp, J., et al., *Human embryonic stem cell-derived oligodendrocyte progenitor cell transplants improve recovery after cervical spinal cord injury.* Stem Cells, 2010. **28**(1): p. 152-63.
15. CLINIC, M. *Stem cell transplant*. [cited 2013 17 December]; Available from: http://www.mayoclinic.com/health/stem-cell-transplant/MY00089/DSECTION=risks.
16. Blesch, A., P. Lu, and M.H. Tuszynski, *Neurotrophic factors, gene therapy, and neural stem cells for spinal cord repair.* Brain Research Bulletin, 2002. **57**(6): p. 833-838.
17. Tuszynski, M.H., et al., *Nerve growth factor delivery by gene transfer induces differential outgrowth of sensory, motor, and noradrenergic neurites after adult spinal cord injury.* Exp Neurol, 1996. **137**(1): p. 157-73.
18. Tuszynski, M.H., et al., *Fibroblasts genetically modified to produce nerve growth factor induce robust neuritic ingrowth after grafting to the spinal cord.* Exp Neurol, 1994. **126**(1): p. 1-14.
19. Grill, R.J., A. Blesch, and M.H. Tuszynski, *Robust growth of chronically injured spinal cord axons induced by grafts of genetically modified NGF-secreting cells.* Exp Neurol, 1997. **148**(2): p. 444-52.
20. Grill, R., et al., *Cellular delivery of neurotrophin-3 promotes corticospinal axonal growth and partial functional recovery after spinal cord injury.* J Neurosci, 1997. **17**(14): p. 5560-72.
21. Xu, X.M., et al., *A combination of BDNF and NT-3 promotes supraspinal axonal regeneration into Schwann cell grafts in adult rat thoracic spinal cord.* Exp Neurol, 1995. **134**(2): p. 261-72.
22. Blesch, A., et al., *Axonal responses to cellularly delivered NT-4/5 after spinal cord injury.* Mol Cell Neurosci,

2004. **27**(2): p. 190-201.
23. English, A.W., W. Meador, and D.I. Carrasco, *Neurotrophin-4/5 is required for the early growth of regenerating axons in peripheral nerves.* Eur J Neurosci, 2005. **21**(10): p. 2624-34.
24. Zuccato, C., et al., *Progressive loss of BDNF in a mouse model of Huntington's disease and rescue by BDNF delivery.* Pharmacological Research, 2005. **52**(2): p. 133-139.
25. Menei, P., et al., *Schwann cells genetically modified to secrete human BDNF promote enhanced axonal regrowth across transected adult rat spinal cord.* Eur J Neurosci, 1998. **10**(2): p. 607-21.
26. Giehl, K.M. and W. Tetzlaff, *BDNF and NT-3, but not NGF, prevent axotomy-induced death of rat corticospinal neurons in vivo.* Eur J Neurosci, 1996. **8**(6): p. 1167-75.
27. NCBI. *CNTF*. [cited 2014 27 Mar]; Available from: http://www.ncbi.nlm.nih.gov/gene?Db=gene&Cmd=ShowDetailView&TermToSearch=1270.
28. Talbott, J.F., et al., *CNTF promotes the survival and differentiation of adult spinal cord-derived oligodendrocyte precursor cells in vitro but fails to promote remyelination in vivo.* Exp Neurol, 2007. **204**(1): p. 485-9.
29. Pernet, V., et al., *Long-distance axonal regeneration induced by CNTF gene transfer is impaired by axonal misguidance in the injured adult optic nerve.* Neurobiology of Disease, 2013. **51**: p. 202-213.
30. Fawcett, J., *Bridging spinal cord injuries.* Journal of Biology, 2008. **7**(7): p. 1-3.
31. Richardson, P.M., U.M. McGuinness, and A.J. Aguayo, *Axons from CNS neurons generated into PNS grafts.* Nature, 1980. **284**(5753): p. 264-265.
32. Davies, S., et al., *Transplanted human astrocytes derived from BMP- or CNTF-treated glial precursors have opposite effects on functional recovery after spinal cord injury.* Cell Transplantation, 2011. **20**(4): p. 552-552.
33. Jones, L.L., et al., *Neurotrophic factors, cellular bridges and gene therapy for spinal cord injury.* Journal of Physiology-London, 2001. **533**(1): p. 83-89.
34. Hersel, U., C. Dahmen, and H. Kessler, *RGD modified polymers: biomaterials for stimulated cell adhesion and beyond.* Biomaterials, 2003. **24**(24): p. 4385-4415.
35. Ruoslahti, E., *RGD and other recognition sequences for integrins.* Annu Rev Cell Dev Biol, 1996. **12**: p. 697-715.
36. Pierschbacher, M.D. and E. Ruoslahti, *Cell attachment activity of fibronectin can be duplicated by small synthetic fragments of the molecule.* Nature, 1984. **309**(5963): p. 30-3.
37. LeBaron, R.G. and K.A. Athanasiou, *Extracellular matrix cell adhesion peptides: functional applications in orthopedic materials.* Tissue Eng, 2000. **6**(2): p. 85-103.
38. Zamir, E. and B. Geiger, *Molecular complexity and dynamics of cell-matrix adhesions.* J Cell Sci, 2001. **114**(Pt 20): p. 3583-90.
39. Geiger, B. and A. Bershadsky, *Assembly and mechanosensory function of focal contacts.* Curr Opin Cell Biol, 2001. **13**(5): p. 584-92.
40. Petit, V. and J.P. Thiery, *Focal adhesions: structure and dynamics.* Biol Cell, 2000. **92**(7): p. 477-94.
41. Pande, G., *The role of membrane lipids in regulation of integrin functions.* Curr Opin Cell Biol, 2000. **12**(5): p. 569-74.
42. Goeldner, M. and R. Givens, *Dynamic Studies in Biology*. 2005: Wiley.
43. Kaplan, J.H., B. Forbush, and J.F. Hoffman, *Rapid photolytic release of adenosine 5'-triphosphate from a protected analog: utilization by the sodium:potassium pump of human red blood cell ghosts.* Biochemistry, 1978. **17**(10): p. 1929-1935.
44. Barth, A., et al., *Time-resolved infrared spectroscopy of intermediates and products from photolysis of 1-(2-nitrophenyl)ethyl phosphates: Reaction of the 2-nitrosoacetophenone byproduct with thiols.* Journal of the American Chemical Society, 1997. **119**(18): p. 4149-4159.
45. Corrie, J.E.T., *Synthesis, photochemistry and enzymology of 2-O-(2-nitrobenzyl)-D-glucose, a photolabile*

derivative of D-glucose. Journal of the Chemical Society-Perkin Transactions 1, 1993(18): p. 2161-2166.

46. Sinha, D.K., et al., *Photocontrol of protein activity in cultured cells and zebrafish with one- and two-photon illumination.* Chembiochem, 2010. **11**(5): p. 653-663.
47. Aujard, I., et al., *o-Nitrobenzyl photolabile protecting groups with red-shifted absorption: Syntheses and uncaging cross-sections for one- and two-photon excitation.* Chemistry-a European Journal, 2006. **12**(26): p. 6865-6879.
48. Cambridge, S.B., et al., *Doxycycline-dependent photoactivated gene expression in eukaryotic systems.* Nature Methods, 2009. **6**(7): p. 527-U86.
49. Salerno, C.P., D. Magde, and A.P. Patron, *Enzymatic synthesis of caged NADP cofactors: Aqueous NADP photorelease and optical properties.* Journal of Organic Chemistry, 2000. **65**(13): p. 3971-3981.
50. Umezawa, N., et al., *Photocontrol of peptide function: backbone cyclization strategy with photocleavable amino Acid.* Chembiochem, 2011. **12**(11): p. 1694-8.
51. Stegmaier, P., J.M. Alonso, and A. del Campo, *Photoresponsive Surfaces with Two Independent Wavelength-Selective Functional Levels.* Langmuir, 2008. **24**(20): p. 11872-11879.
52. Kotzur, N., et al., *Wavelength-Selective Photoactivatable Protecting Groups for Thiols.* Journal of the American Chemical Society, 2009. **131**(46): p. 16927-16931.
53. Furuta, T., et al., *Photochemical properties of new photolabile CAMP derivatives in a physiological saline solution.* Journal of Organic Chemistry, 1995. **60**(13): p. 3953-3956.
54. Furuta, T., et al., *Acyloxycoumarinylmethyl-caged cAMP, the photolabile and membrane-permeable derivative of cAMP that effectively stimulates pigment-dispersion response of melanophores.* Biochemical and Biophysical Research Communications, 1996. **228**(1): p. 193-198.
55. Schade, B., et al., *Deactivation behavior and excited-state properties of (coumarin-4-yl)methyl derivatives. 1. Photocleavage of (7-methoxycoumarin-4-yl)methyl-caged acids with fluorescence enhancement.* Journal of Organic Chemistry, 1999. **64**(25): p. 9109-9117.
56. Hagen, V., et al., *Highly efficient and ultrafast phototriggers for cAMP and cGMP by using long-wavelength UV/vis-activation.* Angewandte Chemie-International Edition, 2001. **40**(6): p. 1046-+.
57. Eckardt, T., et al., *Deactivation Behavior and excited-state properties of (coumarin-4-yl)methyl derivatives. 2. Photocleavage of selected (coumarin-4-yl)methyl-Caged adenosine cyclic 3 ',5 '-monophosphates with fluorescence enhancement.* Journal of Organic Chemistry, 2002. **67**(3): p. 703-710.
58. Bradley, J., D. Reuter, and S. Frings, *Facilitation of calmodulin-mediated odor adaptation by cAMP-gated channel subunits.* Science, 2001. **294**(5549): p. 2176-2178.
59. Wiesner, B., et al., *Cyclic nucleotide-gated channels on the flagellum control Ca2+ entry into sperm.* Journal of Cell Biology, 1998. **142**(2): p. 473-484.
60. Il'ichev, Y.V. and J. Wirz, *Rearrangements of 2-nitrobenzyl compounds. 1. Potential energy surface of 2-nitrotoluene and its isomers explored with ab initio and density functional theory methods.* Journal of Physical Chemistry A, 2000. **104**(33): p. 7856-7870.
61. Schworer, M. and J. Wirz, *Photochemical reaction mechanisms of 2-nitrobenzyl compounds in solution I. 2-nitrotoluene: Thermodynamic and kinetic parameters of the aci-nitro tautomer.* Helvetica Chimica Acta, 2001. **84**(6): p. 1441-1458.
62. Liu, M., et al., *In vitro selection of a photoresponsive RNA aptamer to hemin.* Bioorg Med Chem Lett, 2010. **20**(9): p. 2964-7.
63. Goeldner, M. and R. Givens, *Dynamic studies in biology*. 2006: Wiley.
64. Bosques, C.J. and B. Imperiali, *Photolytic control of peptide self-assembly.* Journal of the American Chemical Society, 2003. **125**(25): p. 7530-7531.

65. Gee, K.R., et al., *Caged bioactive carboxylates. synthesis, photolysis studies, and biological characterization of a new caged N-methyl-D-aspartic Acid.* J Org Chem, 1995. **60**(13): p. 4260-4263.
66. Goubko, C.A., et al., *Hydrogel cell patterning incorporating photocaged RGDS peptides.* Biomed Microdevices, 2010. **12**(3): p. 555-68.
67. Brown, B.B., D.S. Wagner, and H.M. Geysen, *A single-bead decode strategy using electrospray ionization mass spectrometry and a new photolabile linker: 3-Amino-3-(2-nitrophenyl)propionic acid.* Molecular Diversity, 1995. **1**(1): p. 4-12.
68. Casley-Smith, J.R., R.G. Morgan, and N.B. Piller, *Treatment of Lymphedema of the Arms and Legs with 5,6-Benzo-[alpha]-pyrone.* New England Journal of Medicine, 1993. **329**(16): p. 1158-1163.
69. Ramamurthy, V., *Organic molecular photochemistry*. 1999, New York [u.a.]: Marcel Dekker.
70. Givens, R.S. and B. Matuszewski, *Photochemistry of phosphate-esters - an efficient method for the generation of electrophiles.* Journal of the American Chemical Society, 1984. **106**(22): p. 6860-6861.
71. Pinheiro, A.V., P. Baptista, and J.C. Lima, *Light activation of transcription: photocaging of nucleotides for control over RNA polymerization.* Nucleic Acids Research, 2008. **36**(14).
72. Ando, H., et al., *Photo-mediated gene activation using caged RNA/DNA in zebrafish embryos.* Nat Genet, 2001. **28**(4): p. 317-25.
73. Wichterle, O.L., D., *Hydrophilic gels for biological use.* Nature, 1960. **185**: p. 2.
74. Van Vlierberghe, S., P. Dubruel, and E. Schacht, *Biopolymer-based hydrogels as scaffolds for tissue engineering applications: a review.* Biomacromolecules, 2011. **12**(5): p. 1387-1408.
75. Martin, B.C., et al., *Agarose and methylcellulose hydrogel blends for nerve regeneration applications.* J Neural Eng, 2008. **5**(2): p. 221-31.
76. Aymard, P., et al., *Influence of thermal history on the structural and mechanical properties of agarose gels.* Biopolymers, 2001. **59**(3): p. 131-144.
77. Madigan, N.N., et al., *Current tissue engineering and novel therapeutic approaches to axonal regeneration following spinal cord injury using polymer scaffolds.* Respir Physiol Neurobiol, 2009. **169**(2): p. 183-99.
78. Lee, P.Y., et al., *Agarose gel electrophoresis for the separation of DNA fragments.* J Vis Exp, 2012(62).
79. George, E., *Intra-articular hyaluronan treatment for osteoarthritis.* Ann Rheum Dis, 1998. **57**(11): p. 637-40.
80. Mao, J.S., et al., *The properties of chitosan-gelatin membranes and scaffolds modified with hyaluronic acid by different methods.* Biomaterials, 2003. **24**(9): p. 1621-9.
81. Cavallini, G.M., et al., *Comparison of the clinical performance of Healon 5 and Healon in phacoemulsification.* Eur J Ophthalmol, 2002. **12**(3): p. 205-11.
82. Nam, H.S., et al., *Controlled release behavior of bioactive molecules from photo-reactive hyaluronic acid-alginate scaffolds.* Macromolecular Research, 2006. **14**(5): p. 530-538.
83. Pan, L.J., et al., *Viability and differentiation of neural precursors on hyaluronic acid hydrogel scaffold.* J Neurosci Res, 2009. **87**(14): p. 3207-3220.
84. Ren, Y.J., Z.Y. Zhou, and F.Z. Cui, *Hyaluronic acid/polylysine hydrogel as a transfer system for transplantation of neural stem cells.* Journal of Bioactive and Compatible Polymers, 2009. **24**(1): p. 56-62.
85. Wei, Y.T., et al., *Hyaluronic acid hydrogel modified with nogo-66 receptor antibody and poly(L-Lysine) enhancement of adherence and survival of primary hippocampal neurons.* Journal of Bioactive and Compatible Polymers, 2009. **24**(3): p. 205-219.
86. Horn, E.M., et al., *Influence of cross-linked hyaluronic acid hydrogels on neurite outgrowth and recovery from spinal cord injury.* J Neurosurg Spine, 2007. **6**(2): p. 133-40.
87. Goubko, C.A., et al., *Comparative analysis of photocaged RGDS peptides for cell patterning.* J Biomed Mater Res A, 2012.

88. Huang, Y., et al., *Fabrication and in vitro evaluation of the collagen/hyaluronic acid PEM coating crosslinked with functionalized RGD peptide on titanium.* Acta Biomater, 2012. **8**(2): p. 866-877.
89. Ouasti, S., et al., *Network connectivity, mechanical properties and cell adhesion for hyaluronic acid/PEG hydrogels.* Biomaterials, 2011. **32**(27): p. 6456-6470.
90. Cui, F.Z., et al., *Hyaluronic acid hydrogel immobilized with RGD peptides for brain tissue engineering.* Journal of Materials Science-Materials in Medicine, 2006. **17**(12): p. 1393-1401.
91. Kim, J., et al., *Bone regeneration using MMP sensitive-hyaluronic acid based hydrogels*. 2009 35th Annual Northeast Bioengineering Conference. 2009. 42-43.
92. Okabe, K., et al., *Injectable soft-tissue augmentation by tissue engineering and regenerative medicine with human mesenchymal stromal cells, platelet-rich plasma and hyaluronic acid scaffolds.* Cytotherapy, 2009. **11**(3): p. 307-16.
93. Roberts, G.A.F. and K.E. Taylor, *Chitosan gels, 3. The formation of gels by reaction of chitosan with glutaraldehyde.* Die Makromolekulare Chemie, 1989. **190**(5): p. 951-960.
94. Updegraff, D.M., *Semimicro determination of cellulose inbiological materials.* Analytical Biochemistry, 1969. **32**(3): p. 420-424.
95. *Discoveries in plant biology. Volume III*. 2000, Singapore; River Edge, NJ: World Scientific.
96. Bouhadir, K.H., et al., *Sustained and controlled release of daunomycin from cross-linked poly(aldehyde guluronate) hydrogels.* Journal of Pharmaceutical Sciences, 2000. **89**(7): p. 910-919.
97. Bhattacharjee, A. and M. Bansal, *Collagen structure: The Madras triple helix and the current scenario.* Iubmb Life, 2005. **57**(3): p. 161-172.
98. Parenteau-Bareil, R., R. Gauvin, and F. Berthod, *Collagen-based biomaterials for tissue engineering applications.* Materials, 2010. **3**(3): p. 1863-1887.
99. Tedder, M.E., et al., *Stabilized collagen scaffolds for heart valve tissue engineering.* Tissue Engineering Part A, 2009. **15**(6): p. 1257-1268.
100. Surgery, E.o. *Fibrin*. [cited 2014 29 Mar]; Available from: http://www.surgeryencyclopedia.com/Ce-Fi/Fibrin-Sealants.html.
101. Janmey, P.A., J.P. Winer, and J.W. Weisel, *Fibrin gels and their clinical and bioengineering applications.* J R Soc Interface, 2009. **6**(30): p. 1-10.
102. Sahni, A. and C.W. Francis, *Vascular endothelial growth factor binds to fibrinogen and fibrin and stimulates endothelial cell proliferation.* Blood, 2000. **96**(12): p. 3772-8.
103. Lloyd-Williams, P., F. Albericio, and E. Giralt, *Chemical approaches to the synthesis of peptides and proteins*. 1997: CRC PressINC.
104. Merrifield, R.B., *Solid phase peptide synthesis. I. The synthesis of a tetrapeptide.* Journal of the American Chemical Society, 1963. **85**(14): p. 2149-2154.
105. Pennington, M.W. and B.M. Dunn, *Peptide Synthesis Protocols*. 1995: Humana Press.
106. Goubko, C.A. and X.D. Cao, *Patterning multiple cell types in co-cultures: A review.* Materials Science & Engineering C-Materials for Biological Applications, 2009. **29**(6): p. 1855-1868.
107. Cole, M.A., et al., *Stimuli-responsive interfaces and systems for the control of protein-surface and cell-surface interactions.* Biomaterials, 2009. **30**(9): p. 1827-50.
108. Petersen, S., et al., *Phototriggering of cell adhesion by caged cyclic RGD peptides.* Angewandte Chemie-International Edition, 2008. **47**(17): p. 3192-3195.
109. Cheng, X., et al., *Novel cell patterning using microheater-controlled thermoresponsive plasma films.* Journal of Biomedical Materials Research Part A, 2004. **70A**(2): p. 159-168.
110. Majumdar, S., et al., *Novel circular, cyclic and acyclic psi(CH2O) containing peptide inhibitors of SKI-1/S1P:*

synthesis, kinetic and biochemical evaluations. Current Medicinal Chemistry, 2011. **18**(18): p. 2770-2782.

111. Cheng, N. and X.D. Cao, *Photosensitive chitosan to control cell attachment.* Journal of Colloid and Interface Science, 2011. **361**(1): p. 71-78.
112. Basak, A., et al., *A novel enediynyl peptide inhibitor of furin that blocks processing of proPDGF-A, B and proVEGF-C.* Plos One, 2009. **4**(11).
113. Wirkner, M., et al., *Photoactivatable caged cyclic RGD peptide for triggering integrin binding and cell adhesion to surfaces.* Chembiochem, 2011. **12**(17): p. 2623-2629.
114. Friedman, M., *Chemistry, Nutrition, and Microbiology of d-Amino Acids.* Journal of Agricultural and Food Chemistry, 1999. **47**(9): p. 3457-3479.
115. Ruoslahti, E. and M.D. Pierschbacher, *New perspectives in cell adhesion: RGD and integrins.* Science, 1987. **238**(4826): p. 491-7.